CEB REPORT

TVA 10752 (EN DES-2-83)

TITLE: Browns Ferry Nuclear Plant Torus Integrity Long-Term Program Plant Unique Analysis Report			REPORT NO.: CEB-83-34 PLANT/UNIT: BFN Units 1, 2, and 3 SAR SECTION(S):
VENDOR: N/A	CONTRACT No.: N/A	KEY NOUNS: Torus Integrity	UNID SYSTEM(S): Containment Systems
APPLICABLE DESIGN DOCUMENTS: BFN-50-D706, BFN-50-D711	REV: R0	(FOR MEDS USE): 8401090D0018 (392)	MEDS ACCESSION NUMBER: CEB '831221 008
REFERENCES: NUREG-0661, CEB-76-23	R1	840725E0015 (394)	CEB '840712 004
	R2		CEB '841210 008

TENNESSEE VALLEY AUTHORITY

DIVISION OF ENGINEERING DESIGN

CIVIL ENGINEERING SUPPORT BRANCH

	Revision 0	R1	R2
Date	December 21, 1983	7-12-84	12-10-84
Prepared	James K. Rochelle*	JKR *	JKR *
Checked	Stanton T. Drake	STD	STD
Submitted	John S. D. Williams	JSDW	JSDW
Reviewed	Kenneth R. Bayley	KRB	KRB
Recommended	W. A. English	WOE	WOE
Approved	R. O. Bennett	ROB$_{84}$	ROB$_{84}$

*Prepared by CEB, NEB, and BWP representatives, J. K. Rochelle, Lead Engineer; See Acknowledgment.

8502070120 850125
PDR ADOCK 05000259
P PDR

COORDINATION LOG

Document No.: CEB-83-34

Title: BROWNS FERRY NUCLEAR PLANT
TORUS INTEGRITY LONG-TERM PROGRAM PLANT UNIQUE ANALYSIS REPORT

Revision: 2

R–Denotes review

A–Denotes approval

DIVISION OF ENGINEERING AND TECHNICAL SERVICES (DETS)

CEB		EEB		MEB		NEB		QEB		ECB					
R	A	R	A	R	A	R	A	R	A	R	A	R	A	R	A
[illegible]	[illegible]			SDa	SDa	WHB	WRB								
[illegible]	[illegible]			ACR	ACR	DMH	DMH								
LCR	[illegible]			HEC	HEC	WHK	WK								
JAL	[illegible]														
BGR	BGR														
JMM	JMM														

DIVISION OF ENGINEERING PROJECTS NUCLEAR (DEPN)

BFEP		BLEP		IRP		SQEP		WBEP							
R	A	R	A	R	A	R	A	R	A	R	A	R	A	R	A
NRB	NRB														

DIVISION OF ENGINEERING PROJECTS (DEP)

AB		AFP		COP		FEP		HEP		NAP		SEP		TSEP	
R	A	R	A	R	A	R	A	R	A	R	A	R	A	R	A

BPS		IMS		QMS											
R	A	R	A	R	A	R	A	R	A	R	A	R	A	R	A

TABLE OF CONTENTS

TABLE OF CONTENTS (Continued)

TABLE OF CONTENTS (Continued)

TABLE OF CONTENTS (Continued)

TABLE OF CONTENTS (Continued)

TABLE OF CONTENTS (Continued)

TABLE OF CONTENTS (Continued)

TABLE OF CONTENTS (Continued)

TABLE OF CONTENTS (Continued)

LIST OF ILLUSTRATIONS (Continued)

LIST OF ILLUSTRATIONS (Continued)

LIST OF TABLES

LIST OF TABLES (Continued)

LIST OF TABLES (Continued)

LIST OF ABBREVIATIONS

ABBREVIATION	
ABS	Absolute Summation
ACI	American Concrete Institute
ADS	Automatic Depressurization System
AE	Architect/Engineer
AISC	American Institute of Steel Construction
ANSI	American National Standards Institute
ASME	American Society of Mechanical Engineers
ASTM	American Society of Testing Materials
BDC	Bottom Dead Center
BFN	Browns Ferry Nuclear Plant
BWR	Boiling Water Reactor
CFR	Code of Federal Regulations
CH	Chugging
CMM	Consistent Mass Matrix
CO	Condensation Oscillation
DBA	Design Basis Accident
DLF	Dynamic Load Factor
ECCS	Emergency Core Cooling System
EN DES	Ergineering Design
EP	Engineering Procedure
EPRI	Electric Power Research Institute
EQ	Earthquake
F	Fahrenheit
FSAR	Final Safety Analysis Report
FSI	Fluid Structure Iteration
FSTF	Full Scale Test Facility
g	Acceleration due to gravity (32.2 ft/sec^2)
GE	General Electric Company
gpm	Gallons per minute
HPCI	High Pressure Coolant Injection
Hz	Hertz
IBA	Intermediate Break Accident
ksi	Kips per square inch
LDR	Load Definition Report
LOCA	Loss-of-Coolant Accident
LTP	Long-Term Program
MCR	Main Control Room
MS	Main Steam
MSIV	Main Steam Isolation Valve
NOC	Normal Operating Condition
NRC	Nuclear Regulatory Commission

ABBREVIATION (Continued)

OBE	Operating Basis Earthquake
P_b	Primary bending stress
P_L	Local primary membrane stress
P_m	General primary membrane stress
PDM	Pittsburgh Des Moines
psi	Pounds per square inch
psia	Pounds per square inch absolute
psid	Pounds per square inch differential
psig	Pounds per square inch gage
PUAAG	Plant Unique Analysis Application Guide
PUAR	Plant Unique Analysis Report
PULD	Plant Unique Load Definition
Q	Secondary stress due to primary plus bending
QSTF	Quarter Scale Test Facility
RCIC	Reactor Core Isolation Cooling
RHR	Residual Heat Removal
RPS	Reactor Primary System
RPV	Reactor Pressure Vessel
RTD	Resistance Temperature Detectors
S_y	Yield Stress
S_a	Alternating Stress Intensity
S_{an}	Spectral Acceleration
SAC	Structural Acceptance Criteria
SBA	Small Break Accident
SER	Safety Evaluation Report
SORV	Stuck Open Relief Valve
SRSS	Square Root of the Sum of the Squares
S/RV	Safety/Relief Valve
SSE	Safe Shutdown Earthquake
STP	Short-Term Program
TES	Teledyne Engineering Services
TMM	Tributary Mass Matrix
TVA	Tennessee Valley Authority
WRC	Welding Research Council
ZPA	Zero Period Acceleration

Truncation of the downcomers reduces pool swell loads. Addition of S/RV quenchers and RHR return elbow discharge devices ensures stable steam condensation during S/RV blowdowns for all postulated accident conditions. The quenchers also mitigate S/RV discharge loads on the tori for all normal and postulated LOCA events. Finally, addition of the 10-inch S/RV vacuum breakers reduces water clearing loads on the S/RV piping systems for rapid second actuation conditions.

The basic functional requirements for these modifications were defined from generic and plant unique information provided by the Mark I Owners Group and GE and approved by NRC. The other generically approved load mitigation methods were inappropriate or unnecessary for BFN.

1.6.2 Composition of the BFN-PUAR

1.6.2.1 Contents

BFN containment systems are described in Section 2. The new hydrodynamic loads for structural analysis of those systems are summarized in Section 3. Structural analysis of the BFN containment systems and structural design of the necessary plant modifications were performed according to the BFN LTP general design criteria described in Section 4. The five basic categories of structural analysis and design activity are described in Sections 5 through 9.

An evaluation of the bulk and local pool temperatures for various postulated accident conditions was conducted as required by NUREG 0661. Section 10 summarizes the results of that evaluation and describes the new pool temperature monitoring system for each BFN unit.

Section 11 gives a general summary and status of BFN LTP and related modification activities upon submittal of this report for NRC review (on approximately December 31, 1983). It also draws basic conclusions regarding completion of BFN LTP activities for all three BFN units.

Additional information on structural analysis and design methods, as well as confirmatory postmodification S/RV test results, are given in Appendices A through F. Appendix G contains construction photographs of some major BFN LTP modifications. Appendices H and I contain questions and responses resulting from review by NRC's consultants, Brookhaven National Laboratory and Franklin Research Center.

1.6.2.2 Arrangement

The Table of Contents, beginning on page ii, lists the headings and subheadings of each section and appendix. It locates the List of Tables, List of Illustrations, and List of Abbreviations, as well as References.

The title page of each section and appendix is brown, to provide easy access. The text of each section and appendix is numbered separately. For example, page 2-9 is the ninth page in Section 2.

Illustrations include both figures and plates (photographs). All figures and tables are located at the end of each section and appendix, with the exception of Appendices H and I. For example, Figure 2-1 is the first figure in Section 2 and Table A-2 is the second table in Appendix A. Plates are located in Appendix G.

Appendices H and I are arranged in accordance with TVA's October 11, 1984, response to NRC's request for additional information on the BFN PUAR. For each item the arrangement is:

1) Question/request from NRC's consultant

2) TVA's response including tables and figures

Page, table, and figure numbers correspond to the item being addressed. For example, page I-FRC 2-1 is the first page for Franklin Research Center Item 2, and Table BNL 16-3 is the third table for Brookhaven National Laboratory Item 16.

The QBUBS02 code predicts shell pressures which envelop both rigid-wall and flexible-wall test data. It also predicts conservative attenuation rates with time which produce conservative dynamic amplification of torus motion inputs to piping systems and other components attached to the torus.

The first mode frequencies of the vent system downcomers in both the longitudinal and transverse directions were within the frequency range of S/RV discharge air bubbles. Therefore, use of the conservative load attenuation with time according to computer code TQFORBF would result in excessively conservative predictions of downcomer responses. The more realistic attenuation rates of TQFOR03 provided a reasonable drag load definition for combination with other downcomer loads and design of downcomer bracing modifications.

SRSS of multiple valve effects in combination with the conservative aspects of this load definition produced a reasonable analysis and design approach. Absolute summation of multiple valve effects would be excessively conservative because there are 13 S/RV lines discharging into 16 bays of each BFN torus (see Figure 7-3).

Both single and multiple valve tests were run in the S/RV confirmatory test, thereby verifying the overall load interpretation and analytical approach. Load reduction factors were conservatively defined based upon correlation of both single and multiple valve test results (Appendix C).

4.2.3 DBA Condensation Oscillation Hydrodynamic Loads

4.2.3.1 Interpretation

The torus was analyzed for shell pressure harmonic forcing functions at 1-Hz intervals from 1 to 30 Hz. Forcing functions above 30 Hz were neglected.

Referring to Table 4.4.1-2 and Figure 4.4.1-1 of the LDR (Reference 14), the largest input pressure coefficient for each 1-Hz interval was selected from the three alternatives. The response for each interval was determined on the basis of maximum response for any frequency within the 1-Hz band. Then the responses were combined by the following procedure:

1) The responses for four forcing functions (at 4-5 Hz, 5-6 Hz, 10-11 Hz, and 15-16 Hz) were added absolutely.

2) The responses for the other 26 forcing functions were combined by SRSS.

3) The results of 1) and 2) were added absolutely.

DBA condensation oscillation (CO) drag load responses for each structural mode were determined by the same procedure.

4.2.3.2 Justification

This interpretation was developed early in 1980 on the basis of Full Scale Test Facility (FSTF) data analysis by GE and Mark I LTP consultants. That data analysis indicated that input above 30 Hz is of such low energy content as to be negligible in determining torus response. Further, the forcing functions were found to have little or no phase relationship to each other. Very loose phase relationships were seen by one study for forcing functions at 5-6, 10-11, and 15-16 Hz, whereas a more definitive study, Reference 19, showed essentially random phasing of all forcing functions.

The procedure outlined above recognized the remote possibility of constant phase relationships between forcing functions at 5-6, 10-11, and 15-16 Hz. It also recognized the random phasing between all other forcing functions and assured that the desired 84 percent nonexceedance probability was achieved.

Additional conservatisms which were inherent to the BFN DBA CO analysis methods are described in Section 5.4.2.9 and Appendix D.

This interpretation reduced the total calculated response by a factor of 2 or more relative to absolute summation of maximum responses for all 50 forcing functions defined in the LDR. Therefore it eliminated excessive conservatism but ensured a satisfactory nonexceedance probability of the predicted dynamic responses.

4.2.4 Post-Chug Hydrodynamic Loads

4.2.4.1 Interpretation

The torus was analyzed for shell pressure harmonic functions at 1-Hz intervals from 1 to 30 Hz. Forcing functions above 30 Hz were neglected. The dynamic response for each of the 30 forcing functions was calculated separately on the basis of maximum response for any frequency within the 1-Hz band. Then the responses were combined by absolute summation.

Post-chug drag loads were defined and analyzed for harmonic forcing functions at 1-Hz intervals from 1 to 50 Hz. The dynamic responses for each interval were determined on the basis of maximum response for any frequency within the 1-Hz band. Then the combined response for each structural mode was determined by absolute summation of the response for the five largest input coefficients plus SRSS of the other 45 responses.

4.2.4.2 Justification

This interpretation was justified by analysis of FSTF data as documented by Reference 20. The procedure for torus analysis was established and the analysis was performed before completion of Reference 20. By relating Reference 20 results to those obtained by this procedure it was clear that the desired 84 percent nonexceedance probability response was attained. (See Section 5.4.2.11 for a more detailed discussion of this topic.)

The procedure for post-chug drag load on submerged structures is in compliance with the recommendation of Reference 20 for 84 percent nonexceedance probability loading.

Appendix D gives a detailed discussion of the BFN fluid drag load analytical method and identified conservatisms inherent to that method.

This interpretation reduced the analytically predicted responses by a factor of 2 or more relative to the absolute summation of responses for all 50 inputs. Therefore, it eliminated significant excess conservatism from the load definition, but preserved the desired nonexceedance probability.

4.2.5 DBA Pool Swell Hydrodynamic Loads

4.2.5.1 Interpretation

The torus was analyzed for average hydrodynamic pressure loads as defined by the PULD and LDR Section 4.3.2. A 6.5 percent margin was added to predicted responses to account for uncertainties in the test data for both operating and zero ΔP cases.

The vent system and S/RV piping systems in each torus were analyzed for pool swell impact and drag loads at operating and zero ΔP conditions, as defined by R0 of the PULD and the LDR. Zero ΔP velocity, displacement, and circumferential time

delay curves were defined from the 1/4 scale BFN test results. Resulting vent support column reaction time histories for each condition were applied to the torus model in combination with the corresponding pool swell average pressure loads, prior to addition of the 6.5 percent uncertainty margin described above.

Pool swell impact and drag loads for other internal structures were analyzed for one enveloping load case in accordance with LDR Section 4.3.4 and the PULD.

4.2.5.2 Justification

This interpretation was based upon the fact that the 1/12 scale Electric Power Research Institute (EPRI) 3-dimensional test model was a prototypical model of BFN in every significant detail and it was consistent with the BFN 1/4 scale model. This fact eliminated the majority of NRC's concerns expressed in NUREG 0661, which led to specification of an additional 15 percent upload margin and definition of an enveloping longitudinal time delay and velocity distribution for the vent system and other above-pool structures.

The BFN torus was analyzed with a constant effective added fluid mass equal to 80 percent of the total contained fluid mass. The 6.5 percent margin exceeded one standard deviation of the BFN 1/4 scale test data. These considerations ensured an upper bound prediction of torus response, particularly during the upload phase. (See Section 5.4.2.7 for a more detailed discussion in this regard.)

The vent system and S/RV piping systems pool swell impact analysis in the unmodified and modified conditions was completed well before release of NUREG 0661 and subsequent revision of the BFN PULD. The interpretation defined above was more accurate for BFN than that identified by NUREG 0661 Appendix A and it predicted higher impact velocities for the critical regions of the vent header and S/RV piping. Therefore, reanalysis of the BFN vent system and S/RV piping for revised longitudinal variations was not necessary or appropriate. (See Sections 6 and 7 for more discussion of the vent system and S/RV piping analyses.)

Other above-pool structures were conservatively analyzed for one enveloping pool swell impact and drag load case in accordance with NUREG 0661. (Appendix D describes the specific analytical method which was applied.)

6.4 Vacuum Breaker/Main Vent End Cap Intersection

The vacuum breaker valves located on the end cap of the main vent pipes are evaluated in the following paragraphs. Figure 6-6 shows the vacuum breaker/main vent intersection.

6.4.1 Analytical Procedure

6.4.1.1 Analytical Model

The vacuum breaker intersection was modeled using the TPIPE computer program (see Appendix F) for consideration of reactions induced by pool swell vent response and coincident loads. A set of shell pipe intersection spring rates was calculated using Bijlaard procedures from Reference 64. Using the output reactions from the TPIPE model, the shell stresses at the vacuum breaker penetration were determined using the WERCO computer program.

6.4.1.2 Static and Dynamic Loads

Due to location, the load experienced by the vacuum breaker valve varies from the loading imposed on structures previously discussed. The vacuum breaker elevation is such that it is above the water level inside the torus. This significantly reduces the number of phenomena that will act upon the valves. S/RV loads, CO loads, and chugging loads are insignificant at this location, leaving only the effects from pool swell, deadweight, and seismic. Time history data generated by Bechtel Corporation (Reference 17) for the pool swell impact loading analysis was input into the TPIPE model.

6.4.2 Controlling Load Combinations

The number of controlling load combinations required to evaluate this component was reduced to one. Table 6-7 identifies that combination.

6.4.3 ASME Code Allowables

The allowable stress intensities for SA-516 GR 70 carbon steel are shown in Table 6-8. This is consistent with the material composition at the temperature provided in Table 6-3.

6.4.4 Results and Comparisons

The stress experienced by the vacuum breaker/main vent intersection was in large part due to the pool swell impact load. Thus, only combination event 18 from Table 3-1 was required for analysis as seen in Tables 6-7 and 6-8. The calculated stress intensity of 16.7 ksi was well below the Service Level B allowable of 28.95 ksi.

6.5 Vent Header/Downcomer Intersection

The vent header and downcomer pairs typically intersect as shown in the finite element representation which simulated this intersection (Figure 6.6).

6.5.1 Analytical Procedure

6.5.1.1 Analytical Models

The vent header/downcomer intersection was modeled into 45° and 180° beam models for the purpose of evaluating loads described in Section 6.5.2. Flexibility constants were input at adjacent nodes which, when connected, formed a short beam portraying the spring rate of the intersection. Analysis output forces and moments from the beam models were input to a STARDYNE computer code finite element plate and shell model as shown in Figure 6-6. The fine mesh of elements extending around the intersection served to obtain accurate stress output.

6.5.1.2 Static and Dynamic Loads

The loading conditions to which the vent header/downcomer intersection was subjected are identical to those outlined in Section 6.2.1.2.

6.5.2 Controlling Load Combinations

The 27 load combinations were reduced to the controlling combinations shown in Table 6-9.

6.5.3 ASME Code Allowables

The material composition of the vent header/downcomer intersection is SA-516 GR 70 carbon steel. Stress intensity allowable values are listed in Table 6-10.

6.5.4 Results and Comparisons

The results and comparisons presented in this section are products of stress and fatigue evaluations. The fatigue analysis provides information for DBA, SBA, and IBA conditions.

6.5.4.1 Stress Evaluation

The downcomer/vent header stress evaluation was completed using the controlling combinations in Table 6-9. The intersection was most affected by the $P_L + Q$ stress category during the DBA condensation oscillation event from Case 21. The calculated stress intensity of 57.6 ksi, compared to an allowable of 57.9 ksi, could be further reduced by removing thermal expansion since it is a one-time occurrence. The most critical pool swell event combination resulted in a stress intensity of 44.4 ksi as compared to a 45.2 ksi allowable. The SBA chugging combination 15, realizing a $P_L + Q$ stress intensity of 53.3 ksi, could also be reduced by removing the thermal loads as previously mentioned.

6.5.4.2 Fatigue Evaluation

The ASME Code for Class MC requires that a component or structure be evaluated to demonstrate adequate margin against fatigue damage in a cyclic load environment. The approach for this evaluation is to compare maximum stress cycle histogram components with conservative strain cycling fatigue data. The strain cycling data is defined by the fatigue curve in Figure I-9 of the Appendices to the ASME Code. This figure plots the alternating stress intensity (S_a) against the number of allowable cycles which may occur for that particular stress intensity. An analysis for cyclic service is not required for a vessel, component, or structure, provided that Paragraph NE-3221.5d is satisfied for all conditions. The only components of the vent system requiring further evaluation were the downcomer/vent header and downcomer/tiebar intersections and the torus bellows/main vent connection. These three portions of the vent system were critical because of their discontinuity and stress concentration characteristics which resulted in high localized stresses.

Since the occurrence of one accident condition (DBA, SBA, or IBA) and cumulative normal load occurrences was postulated in the fatigue life of the vent system, all three LOCA

events were examined. Table 6-11 presents the usage factors compared with the allowable fatigue usage. Note that thermal transient through-wall stresses were not included in the fatigue evaluation since that stress profile would occur only one time in the design life.

6.6 Vent Pipe Drain

The vent drain is located at the lowest elevation of the head at the end of the main vent inside the wetwell. The drain extends into the water and must be able to withstand the hydrodynamic and accident related loads resulting from a LOCA. The following sections confirm the fact that the drain and modified support configuration shown in Figure 6-8 and described in Section 6.6.5 are qualified.

6.6.1 Analytical Procedure

The vent drain and support were modeled into STARDYNE and a modal analysis was performed. It was determined that the dominant frequency (35.1 Hz) was in a key range for chugging. The resulting loads were evaluated by simple hand calculations.

6.6.2 Controlling Load Combinations

Since the frequency of the vent drain and support is out of the range of the condensation oscillation event, it was determined by inspection that either combinations 11, 16, 18, or 25 would control. Because the structure would be in resonance with key post-chug frequencies, combination 11 (SBA + S/RV + CH) actually controls.

6.6.3 Allowable Stress

The allowable stress for SA-333 GR B carbon steel is 0.66 times the yield stress, or 23.1 ksi, in accordance with Section 4.3.4.

6.6.4 Stress Results and Comparisons

The calculated stress in the new support structure is 21.1 ksi. This is less than the allowable value of 23.1 ksi.

6.6.5 Description of Modifications

The vent pipe drains were truncated to the same elevation as the vent header downcomers, i.e., three feet below minimum pool level. The existing support for each drain was removed

6.7.3 Allowable Stresses

The downcomer/tiebar intersection is made of SA-516 Grade 70 carbon steel. Table 6-13 compares actual stresses derived from the analyses with the ASME and AISC Code allowable stresses per Section 4.3.2 and Section 4.3.4.

6.7.4 Results and Comparisons

6.7.4.1 Stress Evaluation

The downcomer/tiebar intersection was analyzed to Service Level B for Cases 15, 21, 25, and 27. From Tables 6-12 and 6-13, the greatest primary plus secondary stress occurs during the SBA event. The maximum calculated stress intensity was 53.8 ksi, compared to the stress allowable of 57.9 ksi. The largest primary local membrane stress intensity of 27.9 ksi also occurred during the SBA event for Case 15, as compared to a 28.95 ksi allowable stress.

The tiebar itself was further analyzed as a linear support for the loads described in Tables 6-12 and 6-13. As seen from Table 6-14, the most severe stress occurred during the CO event combination at a level of 20.7 ksi. This is below the allowable of 0.66 times the yield stress, or 23 ksi.

6.7.4.2 Fatigue Evaluation

The fatigue evaluation of the downcomer/tiebar intersection is comparable to the evaluation discussed in Section 6.5.4.2. It can be seen from Table 6-11 that the usage factors are well below 1.0, as required.

6.7.5 Description of Modifications

A new tiebar with V-bracing members was required between each downcomer pair to minimize downcomer lateral response induced by condensation oscillation effects. As a result, bending stresses in the vent header/downcomer intersection are reduced and no further reinforcement of that area was required, except as described in Section 6.11.

The tiebar was installed at elevation 534 -0" and the V-bracing members intersect the tiebar at midspan. Fabrication consisted of 3- and 4-inch schedule 40 pipe for the tiebars with short sections of 3-1/2-inch schedule 40 pipe for the bracing at the downcomer end to facilitate field adjustability. All pipe material is ASTM A 53 Grade B or A 106 Grade B.

The connections to the downcomer shell were reinforced using pad plates rolled to match contour and wrapped 120°. The plates were 1/2-inch thick by 7 inches wide for the tiebar connection and 5/8-inch thick by 7 inches wide for the bracing connection. Additional 3/8-inch gussets and small pad plates were provided at the tiebar ends to distribute the loads for adequate structural integrity. A 3/8-inch thick saddle plate was provided at the bracing to tiebar intersection to distribute stresses. All plate material is ASME SA-516 Grade 70. For the configuration, see Figure 6-9 and Plate 9.

6.8 Vent Header Support Columns

6.8.1 Analytical Procedure

The vent header support columns are 8-inch diameter double extra strong pipes attached to the vent header miter bends via pipe collars. Figure 6-2 shows the support columns as they are represented in the computer model. The beams extending from the straight portion of the columns to the vent header are rigid, representing the minimal flexibility of the collars.

6.8.2 Controlling Load Combinations

The 27 design load combinations were reduced to three controlling cases given in Tables 6-15 and 6-16.

6.8.3 Allowable Stresses

The vent column supports are constructed of 8-inch double extra strong A 53 Grade B piping. Table 6-16 compares actual stresses derived from the analysis with AISC stress allowables per Section 4.3.4.

6.8.4 Stress Results and Comparisons

The calculated stresses indicated by Table 6-16 are less than the allowable stress of 16.6 ksi. The combination of events in Table 6-15 are composed of Service Level C loads and compared against Service Level B allowables. The most severe case is due to pool swell impact which imposes a stress of 10.4 ksi. The buckling check evaluates the maximum axial load plus bending moment and shows the highest combined effect occurring for pool swell as expected. The maximum buckling factor is 0.63 compared to a Service Level B allowable of 1.0.

6.9 Vent System Miter Bends

There are three structural areas in the vent system at which miter bends are located. The main vent, vent header, and downcomer miter bends are all Class MC components. However, for analysis purposes these items lend themselves more to treatment as piping components. Paragraph NB-3680 was introduced for stress evaluation while retaining the Class MC allowables. The following subsections summarize the analysis of these three types of miter bends.

6.9.1 Analytical Procedure

As mentioned above, the ASME Code provides a guide for the evaluation of miter bends. The modeling of the bends is indicated in Figure 6-2. Stress intensification factors are presented in Table 6-21. These stress intensification factors were calculated using the vent system beam model in conjunction with results from the Bechtel analysis, which provided detailed modeling of the miters in question. Maximum primary plus secondary stresses were ratioed to the nominal section stresses generated from the beam model thereby defining the stress intensification factors.

6.9.2 Controlling Load Combinations

The three controlling load combinations are shown in Tables 6-17, 6-18, and 6-19.

6.9.3 ASME Code Allowables

The ASME Code allowable stresses are presented in Tables 6-17, 6-18, and 6-19.

6.9.4 Stress Results and Comparisons

The main vent miter bend was evaluated for three load cases using Service Level C loads and Service Level B allowables. As seen from Table 6-17, these stresses are considerably below the allowables, showing a maximum value of 3.9 ksi, compared with a 28.95 ksi allowable for the condensation oscillation event combination.

In the same manner, the vent header miter bend and the downcomer miter bend were evaluated for three cases, each involving CO, chugging, and pool swell (Tables 6-18 and 6-19). The maximum local membrane stresses for the Service

Level C loading on the miter bends were found to be 18.6 ksi and 20.7 ksi, respectively. When compared with the Service Level B allowable of 28.95 ksi, these areas are qualified.

6.10 Torus Bellows

The torus bellows are flexible expansion joints allowing movement of the main vent pipes through the torus wall while maintaining the required pressure boundary. The analysis performed on this structure was done in accordance with Standards of the Expansion Joint Manufacturer's Association, Inc., (Reference 24). Fatigue life is the dominant concern.

6.10.1 Analytical Procedure

6.10.1.1 Analytical Model

The flexibility of the bellows was the concern in accurately representing the bellows in the 45° and 180° beam models. In Figure 6-2, local springs were inserted. Output from the 45° and 180° models in the form of displacements was extracted from the various loading events. The combination of these cases as described in Section 6.10.2 was then used to calculate stresses in the bellows.

6.10.1.2 Static and Dynamic Loads

The loading events to which the torus bellows are subjected are explained in Section 6.2.1.2.

6.10.2 Design Loading Conditions

The controlling loading conditions were provided by Reference 21 for SBA, IBA, and DBA events.

6.10.3 ASME Code Allowables

The ASME Code makes reference to bellows in Paragraph NE-3365. Standards of the Expansion Joint Manufacturer's Association, Inc., offers a more straightforward and acceptable approach for fatigue evaluation of bellows.

6.10.4 Results and Comparisons

Results of the fatigue evaluation are shown in Table 6-12 of Section 6.5.4. No significant usage factor is observed. Therefore, the fatigue failure of these components does not present a significant concern.

TABLE 6-9

CONTROLLING LOAD COMBINATIONS AND SERVICE LEVELS OF DOWNCOMER/VENT HEADER INTERSECTION

EVENT	COMBINATION	SERVICE LEVEL
21	DBA + SSE EQ + CO	B
27	DBA + SSE EQ + S/RV + CO	B
25	DBA + SSE EQ + S/RV + PS	C
18	DBA + OBE EQ + PS	B
15	SBA + SSE EQ + S/RV + CH	B
15	SBA + SSE EQ + S/RV + CH	B

TABLE 6-10

MAXIMUM STRESS INTENSITIES ON DOWNCOMER/VENT HEADER INTERSECTION

EVENT	STRESS CATEGORY	STRESS	ALLOWABLE
21	$P_L + Q$	57.60 KSI	57.9 KSI
27	P_L	14.6	37.6
25	P_L	44.4	45.2
18	P_L	31.4	37.6
15	$P_L + Q$	53.3	57.9
15	P_L	21.6	37.6

TABLE 6-11

FATIGUE USAGE FACTORS
FOR CONTAINMENT VENT SYSTEM

COMPONENT	ALLOWABLE FATIGUE USAGE	DBA USAGE	SBA/IBA USAGE
DOWNCOMER / VENT HEADER INTERSECTION	1.0	.559	.610
DOWNCOMER / TIEBAR INTERSECTION	1.0	.107	.353
TORUS BELLOWS INTERSECTION	1.0	.000	.000

TABLE 6-12

CONTROLLING LOAD COMBINATIONS AND SERVICE LEVELS OF DOWNCOMER/TIEBAR INTERSECTION

EVENT	COMBINATION	SERVICE LEVEL
21	DBA + SSE EQ + CO	B
27	DBA + SSE EQ + S/RV + CO	C
21	DBA + SSE EQ + CO	B
25	DBA + SSE EQ + S/RV + PS	B
15	SBA + OBE EQ + S/RV + CH	B
15	SBA + SSE EQ + S/RV + CH	B

TABLE 6-13

MAXIMUM STRESS INTENSITIES ON DOWNCOMER/TIEBAR INTERSECTION

EVENT	STRESS CATEGORY	STRESS	ALLOWABLE
21	P_L	21.7 KSI	28.95 KSI
27	P_L	30.6	34.74
21	$P_L + Q$	30.9	57.9
25	P_L	28.4	28.95
15	$P_L + Q$	53.4	57.9
15	P_L	27.97	28.95

TABLE 6-14
STRESS EVALUATION ON TIEBAR

EVENT	STRESS CATEGORY	STRESS	ALLOWABLE
27	P_L	20.7 KSI	23 KSI
25	P_L	8.7	23
15	P_L	18.0	23

TABLE 6-15

CONTROLLING LOAD COMBINATIONS AND SERVICE LEVELS OF THE VENT COLUMN SUPPORTS

EVENT	COMBINATION	SERVICE LEVEL
27	DBA + SSE EQ + S/RV + CO	B
25	DBA + SSE EQ + S/RV + PS	B
15	SBA + SSE EQ + S/RV + CH	B

TABLE 6-16

STRESS AND BUCKLING EVALUATION ON VENT COLUMN SUPPORTS

EVENT	STRESS CATEGORY	STRESS	ALLOWABLE	BUCKLING FACTOR
27	P_L	7.1 KSI	16.6 KSI	.43
25	P_L	10.4	16.6	.63
15	P_L	7.6	16.6	.46

TABLE 6-17
MAXIMUM STRESS INTENSITIES ON
MAIN VENT MITER BEND

EVENT	STRESS CATEGORY	STRESS	SERVICE LEVEL	ALLOWABLE
27	P_L	3.9 KSI	B	28.95 KSI
25	P_L	1.8	B	28.95
15	P_L	2.4	B	28.95

TABLE 6-18
MAXIMUM STRESS INTENSITIES ON
VENT HEADER MITER BEND

EVENT	STRESS CATEGORY	STRESS	SERVICE LEVEL	ALLOWABLE
27	P_L	18.0 KSI	B	28.95 KSI
25	P_L	15.5	B	28.95
15	P_L	18.7	B	28.95

TABLE 6-19
MAXIMUM STRESS INTENSITIES ON
DOWNCOMER MITER BENDS

EVENT	STRESS CATEGORY	STRESS	SERVICE LEVEL	ALLOWABLE
27	P_L	16.5 KSI	B	28.95 KSI
25	P_L	13.8	B	28.95
15	P_L	20.6	B	28.95

TABLE 6-20

STRESS EVALUATION AT KEY LOCATIONS FOR ZERO ΔP
(LOAD COMBINATION P + W + T + PS ZERO ΔP)

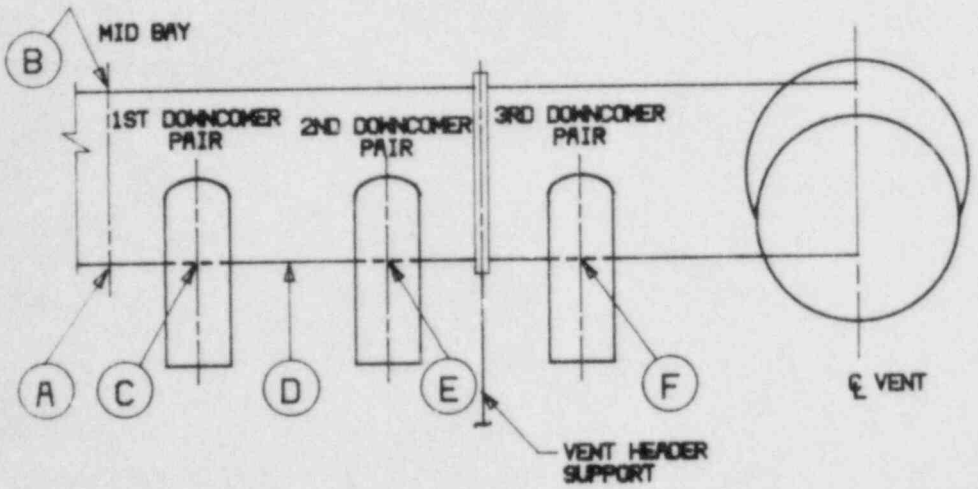

LOCATION	STRESS INTENSITY	CALCULATED STRESS (KSI)	ALLOWABLE STRESS (KSI)	BUCKLING INTERACTION $\frac{\sigma_L}{\sigma_{LA}} + \frac{\sigma_H}{\sigma_{HA}} \leq 1.0$
MIDBAY BOTTOM ELEMENT 13	P_M	12.0	41.6	
	$P_L + P_b$	28.1	62.5	
	σ_L	12.0	25.5	
Ⓐ	σ_H	3.1	16.9	0.7
MIDBAY TOP ELEMENT 1	P_M	8.0	41.6	
	$P_L + P_b$	17.8	62.5	
	σ_L	4.6	25.5	0.2
Ⓑ	σ_H	0.5	16.9	
BOTTOM BETWEEN 1ST D/C PAIR ELEMENT 1062	P_M	9.0	41.6	
	$P_L + P_b$	41.2	62.5	
	σ_L	11.0	25.5	
Ⓒ	σ_H	0.7	16.9	0.5
BOTTOM BETWEEN TWO PAIRS OF D/C ELEMENT 1438	P_M	15.5	41.6	
	$P_L + P_b$	24.1	62.5	
	σ_L	13.9	22.5	
Ⓓ	σ_H	0.7	13.6	0.7
BOTTOM BETWEEN 2ND D/C PAIR ELEMENT 2062	P_M	17.4	41.6	
	$P_L + P_b$	41.6	62.5	
	σ_L	17.2	22.5	
Ⓔ	σ_H	3.4	13.6	1.0
BOTTOM BETWEEN 3RD D/C PAIR ELEMENT 3062	P_M	5.3	41.6	
	$P_L + P_b$	19.4	62.5	
	σ_L	5.0	22.5	
Ⓕ	σ_H	1.7	13.6	0.3

TABLE 6-21
STRESS INTENSIFICATION FACTORS

LOCATION	FACTOR
MAIN VENT MITER BEND	3.85
VENT HEADER MITER BEND	8.2
DOWNCOMER MITER BEND	3.82

TABLE 7-1
DRYWELL LOAD COMBINATIONS

LOADS	DEADWEIGHT	PRESSURE	THERMAL (1)	NOC S/RV (2)	IBA S/RV (3)(6) (SUBSEQUENT ACTUATION, STEAM IN DRYWELL)	OBE (4)	SSE (4)	POOL SWELL (5)	SERVICE LEVEL
CASE 1	X	X	X	X		X			B
CASE 2	X	X		X			X		C
CASE 3	X	X			X		X		D
CASE 4	X	X		X			X	X	D

1. WORST CASE THERMAL EXPANSION
2. WORST CASE FIRST ACTUATION VS. SUBSEQUENT ACTUATION.
3. IBA S/RV SUBSEQUENT ACTUATION, STEAM IN DRYWELL.
4. SEISMIC EVENTS INCLUDE ANCHOR MOVEMENTS.
5. POOL SWELL INCLUDES VENT RESPONSE AND DISPLACEMENT.
6. EVALUATION OF PRELIMINARY ANALYSIS INDICATED SBA/IBA FIRST AND SECOND ACTUATIONS WITH AIR IN THE DRYWELL TO BE LESS SEVERE THAN NOC BLOWDOWNS. WITH THE EXCEPTION OF SUBSEQUENT ACTUATION, STEAM IN THE DRYWELL, THE NOC BLOWDOWNS ENVELOPE SBA/IBA BLOWDOWNS. BECAUSE OF THE LOW PROBABILITY OF STEAM IN THE DRYWELL COINCIDENT WITH MAX REFLOOD, ACTUATION UNDER THESE CONDITIONS IS ASSUMED TO BE SERVICE LEVEL D.

TABLE 7-2

NOC - SERVICE LEVELS B AND C LOAD COMBINATIONS

LOADS	DEADWEIGHT	PRESSURE	NOC S/RV (1) 1ST. ACTUATION EVENTS	NOC S/RV (1) 2ND ACTUATION EVENTS	SSE	SERVICE LEVEL
CASE 1	X	X	X			B
CASE 2	X	X		X		B
CASE 3	X	X	X		X	C
CASE 4	X	X		X	X	C

1. S/RV ACTUATION EVENTS INCLUDE TORUS RESPONSE, FLUID DRAG ON SUBMERGED STRUCTURES, BLOWDOWN FORCE IN PIPE AND QUENCHER WATER CLEARING THRUST

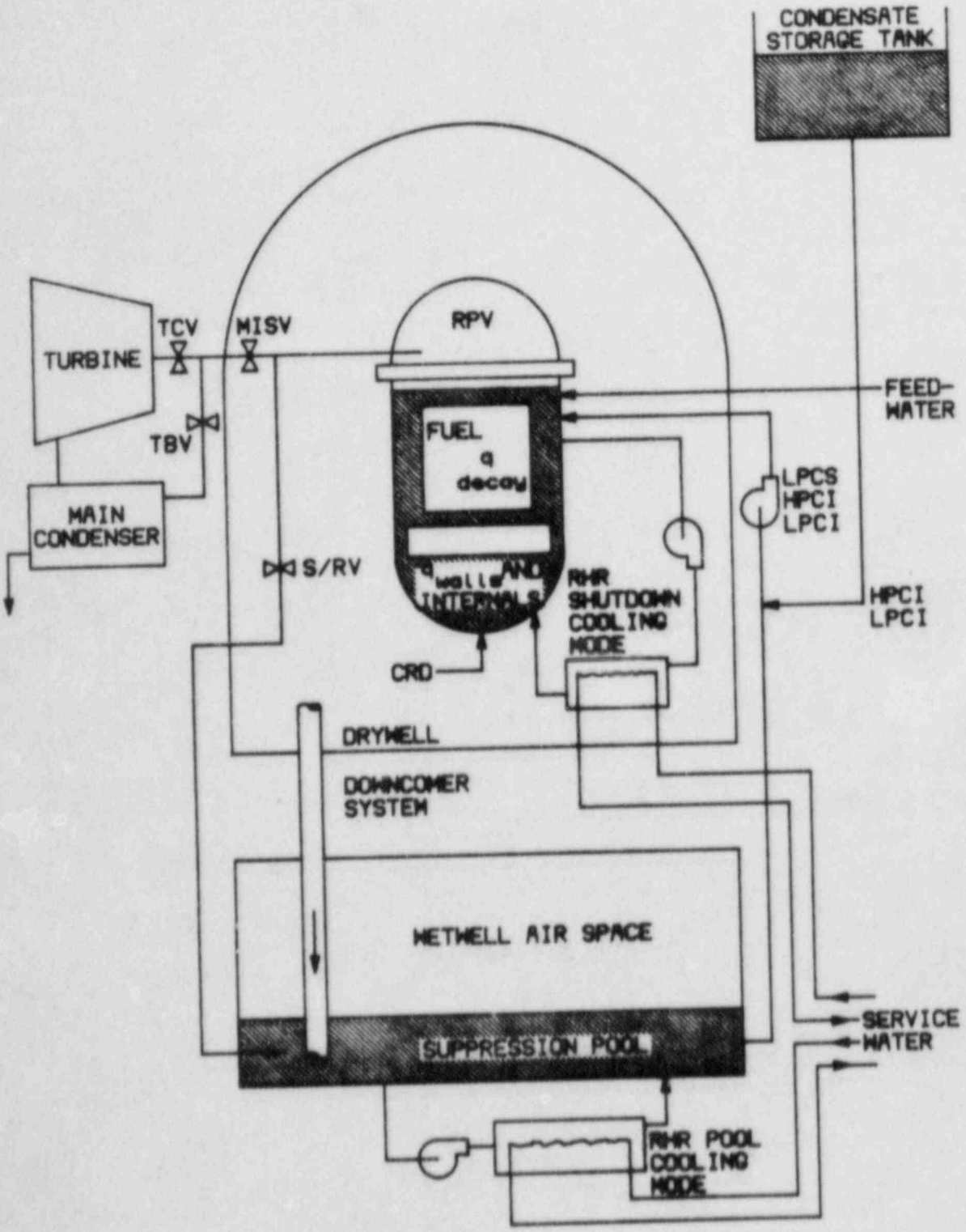

FIGURE 10-1
COUPLED REACTOR AND SUPPRESSION POOL MODEL

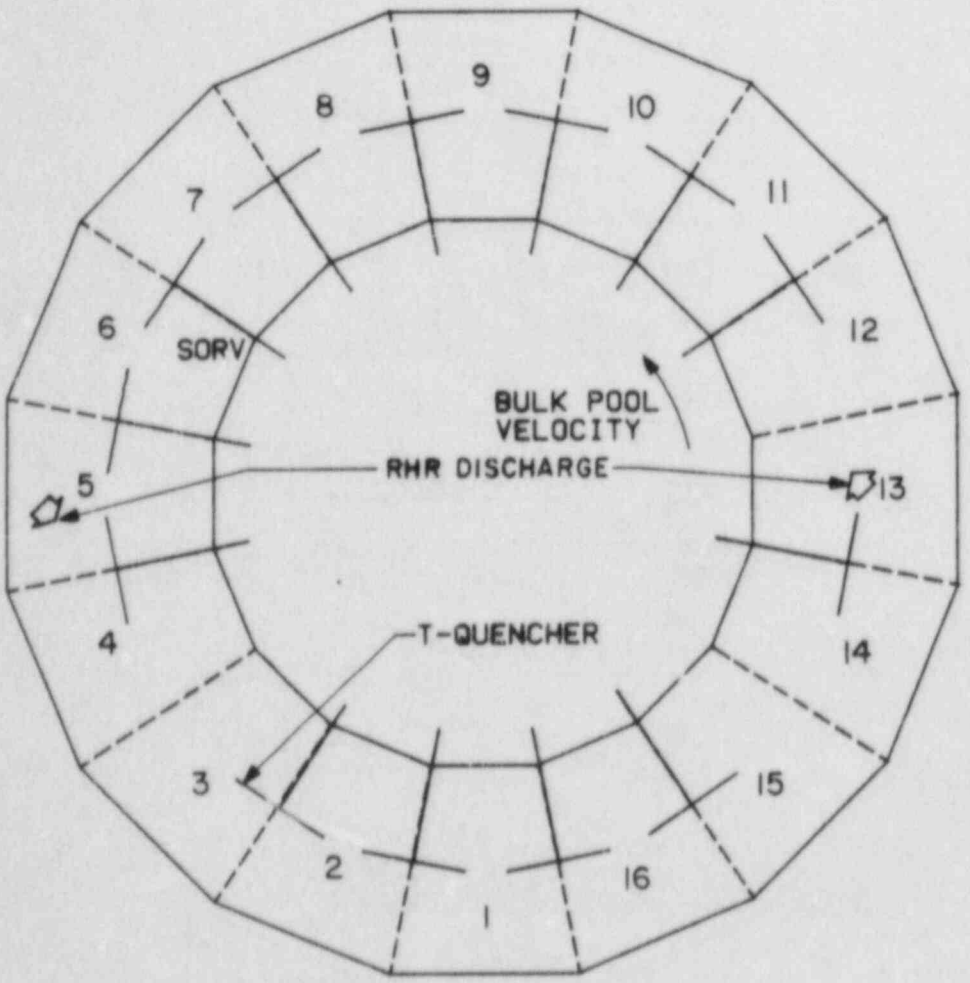

FIGURE 10-2

PLAN VIEW OF BROWNS FERRY SUPPRESSION POOL WITH T-QUENCHERS AND RHR DISCHARGE LOCATIONS USED IN THE LOCAL POOL TEMPERATURE MODEL

11.0 SUMMARY AND CONCLUSIONS

11.1 General

The BFN Torus Integrity LTP has been underway since 1977. The program objective was to upgrade the containment systems of each BFN unit for suppression pool hydrodynamic loads which were not explicitly included in the original design specification.

Mark I Owners Group and NRC activities resulted in generic load definitions and corresponding structural acceptance criteria to be applied for each domestic Mark I plant. NRC's generic safety evaluation report for the Mark I containment system long-term program, NUREG 0661 (Reference 1), was published in July 1980.

The current orders for completion of BFN LTP modifications were issued on January 19, 1982. Those orders require installation of all modifications necessary for compliance with NUREG 0661 before the start of Cycle 6 operations of each BFN unit.

11.2 Browns Ferry Design Criteria

The BFN LTP general design criteria (Section 4.0) defined the basis for structural analysis of BFN containment system components as well as structural design of required modifications. It also ensured compliance with the intent of NUREG 0661.

The detailed design criteria for analysis of torus attached piping systems (Appendix A) supplemented the general design criteria and defined specific requirements and procedures for analysis of torus attached piping systems.

11.3 Structural Analyses and Design of Required Modifications

Structural analysis and design of required modifications for each basic category of BFN containment system components were performed as described in Sections 5.0 through 9.0. The analyses addressed containment systems as configured for the start of Cycle 6 operations of each unit, including plant modifications installed for NUREG 0661 compliance and for other reasons. Modifications related to suppression pool local and bulk temperature requirements in NUREG 0661 were designed as described in Section 10.0. All modification designs complied with the Browns Ferry LTP design criteria and NUREG 0661.

Analysis and design of associated modifications to the 10-inch S/RV discharge line vacuum breakers and the drywell/wetwell vacuum breakers have also been completed.

Permanent documentation of all analysis and design activities associated with the BFN LTP was accomplished, in compliance with Section 4.6.

Future modifications to BFN containment system components will be designed in accordance with the BFN LTP design criteria, when the modifications are within the region of influence of torus hydrodynamic loads.

11.4 S/RV Confirmatory Test

An in-plant S/RV confirmatory test was successfully completed in BFN Unit 2 during April 1983 in accordance with Section 4.6. The test results were documented by Reference 41. Correlation of analysis and test results, including definition of selected load reduction factors, was accomplished as described in Appendix C.

11.5 Installation of Modifications and Final Conclusions

At this time (December 1984), all LTP modifications and 10-inch S/RV vacuum breaker modifications have been installed in BFN Units 1 and 3. Major LTP modifications and 10-inch S/RV vacuum breaker modifications have been installed in Unit 2. Unit 2 is in its Cycle 6 refueling outage.

All BFN containment system modifications for compliance with NUREG 0661 will be completed before restart for Cycle 6 operations, in accordance with NRC's orders (Reference 12). Other modifications will be installed according to a NRC-approved integrated schedule.

BFN LTP total costs are currently estimated at $105,000,000 excluding interest payments and lost power revenues while installing modifications. The extent and scope of those modifications are summarized by Table 11-1 and the construction photographs in Appendix G.

This PUAR provides an accurate and sufficient summary of LTP activities for all three BFN units.

TABLE A-4 (CONTINUED), SHEET 8
ANALYSIS CRITERIA FOR TORUS ATTACHED PIPING-LOCA EFFECTS (1, 2, 5)

DBA (CONTINUED)

PLANT CONDITION (LOAD SOURCE TYPE)	MOMENT CONSTITUENTS FROM LOAD SOURCES	EQUATIONS AND STRESS LIMITS
POSTPROCESSOR 8 PUAAG COMB. 16 0.0 POOL SHELL **PRIMARY** (PRESSURE + SUSTAINED + DBA) NONESS.-SVC LEVEL D ESS. - SVC LEVEL B	$M_A = M\ (DW + PL)$ $M_{BF} = M[(P_2 + (APID \text{ OR } PSF) + FI + PSDL + PSFB + DMJDL]$	$\frac{P_{max} d^2}{(D_o^2 - d^2)} + \frac{0.75 i (M_A + M_{BF})}{Z} \leq 2.4\ S_h$ ESSENTIAL & NONESS. $\leq 1.2\ S_h$ ACT.COMP. $P_{max} \leq 2.0$ P NONESS. ≤ 1.1 P ESS.
SECONDARY (PRESSURE + SUSTAINED +EXPANSION + DBA)	$M_C = M(T_1 + PS2 + PQ2)$ $i = 1.2$ OR $M_C = M[T_1]$ AND $M_D = M[PS2 + PQ2]$	$\frac{P_d^2}{(D_o^2 - d^2)} + \frac{0.75 i M_A}{Z} + \frac{i M_B}{Z} \leq S_A + S_h$ OR $\frac{i M_C}{Z} \leq S_A$ $\frac{i M_D}{Z} \leq 3 S_c$

TABLE A-4 (CONTINUED), SHEET 9

NOTES:

1. THESE EQUATIONS REPRESENT THE WORST CASES FROM PUAQC TABLE 5-2 AND MARK I CONTAINMENT PROGRAM LOAD DEFINITION REPORT NEDO-21888,SECTION 3, TABLE 3.0-3, FIGURES 3.0-1, -2, -3, -4, AND -5.

2. ALL DYNAMIC ANCHOR POINT MOVEMENTS ARE INCLUDED IN EQUATIONS 9, 10, AND 11. FATIQUE ANALYSIS REQUIREMENTS WILL BE SATISFIED BY DEMONSTRATION OF COMPLIANCE WITH ASME CODE SECTION III NC 3600, EQUATIONS 9, 10, AND 11.

3. THE PUAAQ (REFERENCE 13) PERMITS THE PIPING STRESS ALLOWABLES, PIPING DAMPING VALUES, AND PIPING SUPPORT ALLOWABLES TO MEET THE REQUIREMENTS OF SERVICE LEVEL C. THIS DOES NOT APPLY TO ACTIVE COMPONENTS.

4. THE PUAAQ (REFERENCE 13) PERMITS THE PIPING STRESS ALLOWABLES, PIPING DAMPING VALUES, AND PIPING SUPPORT ALLOWABLES TO MEET THE REQUIREMENTS OF SERVICE LEVEL D. THIS DOES NOT APPLY TO ACTIVE COMPONENTS.

5. A STRESS RANGE EVALUATION MUST BE PERFORMED FOR ALL THERMAL CYCLIC CONDITIONS AND ALL DYNAMIC DISPLACEMENT CYCLIC CONDITIONS THAT ARE QUALIFIED BY CODE EQUATIONS 10 OR 11.

BFN-PUAR

APPENDIX H

FINAL TVA RESPONSES TO NRC AND BROOKHAVEN NATIONAL LABORATORY QUESTIONS

General Response to PUAR Questions

BFN LTP analysis and design activity has proceeded on a schedule necessary to support installation of all modifications during the Cycle 4 and 5 refueling outages of each unit, as required by NRC. The first BFN Cycle 4 refueling outage began in April 1981, and most of the major modification designs were complete by May 1981. Remaining modification designs, primarily for torus attached piping external supports, were complete in time to support installation during the Cycle 5 refueling outages.

In order to satisfy schedule commitments, it was necessary to make interpretations of LDR and NUREG 0661 requirements based upon the best available information at the time of analysis. Most of the interpretations were originally established in 1979 and early 1980. A continuing effort to remove excessive conservatism from load definitions and analysis methods was made, particularly when that conservatism would result in unnecessary, impractical modifications.

When later information on load definitions and associated analysis methods became available, it was compared to the previous interpretations. The later information was used for reanalysis and associated design work if a significant unconservatism in the previous interpretation was indicated. For example, the final downcomer tiebar/V-bracing modification resulted from November 1981 changes in the DBA condensation oscillation lateral load definition.

Sometimes, later information was used to remove excessive conservatism in remaining analysis and design work. For example, the 1.1 SRSS load combination technique was permitted for torus attached piping analysis after NRC's final position on this subject was defined in April 1983 by PUAR Reference 58. An absolute summation combination technique was required prior to that time.

Finally, when the later information showed the previous load definitions and analysis methods to be adequately (but not excessively) conservative, the original interpretations were retained. In these situations, reanalysis utilizing the later information would have been unnecessary and costly, and, in some cases, would have resulted in delays in the installation of modifications.

Many of the PUAR questions derive from situations where the original interpretations stated in PUAR Section 4 were used for analysis. Justification for these interpretations was provided in PUAR Section 4, Section 5, and Appendix C. Additional technical justification follows in the responses to specific questions on these topics. Other PUAR questions simply request additional information, which is provided in the responses.

It is TVA's position that the BFN PUAR and our review question responses demonstrate compliance with the intent of the Mark I Containment Long-Term Program and NUREG 0661 (i.e., to upgrade the containment system safety margins, for all postulated hydrodynamic loading conditions, to those intended by the original design specifications). On this basis, we feel that all indicated safety concerns are fully and satisfactorily addressed, and we respectfully request a favorable final evaluation for the BFN LTP.

ITEM 1:

According to Section 4.2.5 of the PUAR, BFN used the loads defined by the PULD and the LDR Section 4.3.2 for pressure loads on the torus. However, BFN applied a much smaller margin on the LDR load than stipulated in NUREG 0661, page A-6.

The BFN margin of 6.5 percent on the LDR upload is justified in the BFN PUAR on the basis that the 15 percent margin recommended on page 39 of NUREG 0661 is unnecessary because the EPRI 1/12-scale model had the BFN geometry, and that the Acceptance Criteria (AC) margin of 21.5 percent should therefore be reduced by 15 percent to yield 6.5 percent. This does not meet the intent of the AC. The 15 percent margin of NUREG 0661 was imposed for several reasons (see pp. 36-38 of NUREG 0661), the geometry being only one of the concerns. Consequently, a full justification for the reduction of the margin from 21.5 percent to 6.5 percent is needed, or the ability of the torus to withstand a 15 percent load increase must be demonstrated.

RESPONSE:

The uncertainty margins used for BFN pool swell load definition and the BFN pool swell analysis procedure ensured conservative structural response predictions. Some justification for this fact is given in Section 4.2.5.2 of the PUAR. Additional justification follows:

1. Uncertainties regarding the 2D/3D test model results were minimized because the 1/4 scale 2D and 1/12 scale 3D models for the generic Mark I LTP tests were prototypical of BFN geometry.

2. Significant conservatism was added to the BFN pool swell load definition because fluid compressibility effects in the vent system were not considered in the 1/4 scale plant unique tests. This conservatism is recognized and quantified in Section 2.4 of Supplement 1 to NUREG 0661.

3. BFN plant unique 1/4 scale tests for normal operating conditions were conducted at minimum ΔP and maximum downcomer submergence, thereby ensuring upper-bound pool swell load predictions.

4. BFN plant unique 1/4 scale tests for 0.0 ΔP conditions were conducted at 0.0 ΔP and maximum downcomer submergence, thus ensuring upper-bound pool swell load predictions.

5. The BFN vent system and torus analysis procedures for pool swell loading included significant conservatisms. Sections 4.4.5 and 6.11 of the PUAR summarize the BFN vent system analysis procedure. Sections 4.4.4 and 5.4.2.7 of the PUAR summarize the BFN torus analysis procedure. Significant analytical conservatisms included the two percent damping assumption for vent system analysis, the 80 percent water mass assumption for torus analysis, and the two percent torus damping assumption for all operating ΔP pool swell load combinations.

6. The BFN uncertainty margin for pool swell loads (6.5 percent) was conservatively applied to the predicted torus response including vent system input effects, whereas the download and upload margins in NRC's acceptance criteria (Appendix A of NUREG 0661) are applicable for torus hydrodynamic pressure loads only.

7. The BFN uncertainty margin (6.5 percent) exceeds NRC's recommended download margin (5.4 percent). It also exceeds one standard deviation of the BFN 1/4 scale results for operating ΔP conditions. Those standard deviations were approximately 3.6 percent and 4.0 percent for upload and download respectively.

8. BFN operating ΔP pool swell dynamic responses were conservatively combined with dynamic responses from other load sources by the methods described in Section 4.4.2 of the PUAR.

Additional assurance regarding any remaining upload concern is provided by the fact that the BFN torus tiedown design is not controlled by a pool swell load combination. This would remain true even if an additional 15 percent upload margin were added for pool swell loads.

ITEM 2:

What margin was applied on the LDR download? Is the download specification consistent with Section 2.3 of the the Acceptance Criteria?

RESPONSE:

A 6.5 percent uncertainty margin was applied for both download and upload as described in the response to BNL item 1. The specification in Section 2.3 of NRC's acceptance criteria requires a download margin of 5.4 percent, based upon a peak download of 2700 pounds for BFN 1/4 scale operating ΔP tests.

ITEM 3:

For what structures would the load exceed acceptable levels if the torus pressure loads were made consistent with NUREG 0661? By how much, and for what load combinations?

RESPONSE:

To make the BFN torus pressure loads consistent with NUREG 0661 an additional 15 percent margin would be added to the upload phase--if the other conservatisms in the BFN pool swell load definition were disregarded. The download margin would be reduced by 1 percent. Assuming that the same conservative analytical procedure was applied, maximum stresses in the download phase would decrease slightly and maximum stresses in the upload phase would increase by less than 15 percent. (An increase of 5 to 10 percent is estimated.) This level of potential stress increase could readily be compensated by removal of some of the conservatism in the analytical procedure and load combination technique. Therefore, realistically, there is no potential to overstress a BFN structure by changing the torus pressure load definition to comply with NUREG 0661 generic margins.

ITEM 4:

Was the vent header impact load definition of pages 6-17 of the PUAR in accordance with Section 2.10.1 of NUREG 0661? If not, explain the differences and provide estimates showing that sufficient margin exists to accommodate the NUREG load.

RESPONSE:

The vent header impact load definition was not in accordance with Section 2.10.1 of the NUREG 0661 acceptance criteria. Section 2.10.1 addresses loads on a vent header deflector. BFN does not have a vent header deflector; however, the BFN vent headers were reinforced near the center of each non-vent bay as a result of pool swell impact loading analysis as described in Section 6.11.3 of the PUAR. A typical BFN header reinforcement installation is shown by PUAR Plates 7 and 8.

The BFN vent system pool swell impact load analysis (PUAR Reference 17) and header reinforcement modification design were performed in 1979, prior to the release of NUREG 0661. The longitudinal velocity and impact timing profiles were based upon EPRI 1/12 scale split orifice tests for operating ΔP and 0.0 ΔP pool swell conditions.

NUREG 0661 specified the use of a single "conservative" profile for impact velocity and timing for all conditions. However, a comparison of the resulting peak impact pressures on the BFN vent header showed that the existing analytical values were more conservative for the entire non-vent bay. This was particularly true in the critical region where the BFN reinforcement modification is located. Therefore, within the non-vent bay it was concluded that the existing analysis results were conservative relative to the revised load definition from NUREG 0661.

Within the vent bay the peak impact pressures would be somewhat higher with the revised load definition. However, conservative estimates of the increased vent system stresses in this region showed all stresses to be less than 24 percent of allowables for the operating ΔP case and 37 percent for the 0.0 ΔP case.

Further consideration of this information leads to the basic conclusion that the 1979 analysis was appropriately conservative and sufficiently accurate to address all structural concerns of the BFN vent system for pool swell impact and drag loads. Additional analysis was not necessary.

ITEM 5:

Were the LOCA jet and bubble drag loads for BFN evaluated in accordance with the LDR and NUREG 0661?

RESPONSE:

Yes, LOCA jet and bubble drag loads for BFN were evaluated in accordance with the LDR and NUREG 0661 (See PUAR, Appendix D, Sections D.1.1.2 and D.1.1.1, respectively, for discussions).

ITEM 6:

For analyzing structures affected by CO loads, the LDR and NUREG 0661 prescribe absolute summation of the CO load harmonics at 1-Hz intervals from 1 to 50 Hz. BFN used an alternate approach where:

(i) forcing frequencies above 31 Hz were neglected, and

(ii) four particular load harmonics (the ones at 4-5, 5-6, 10-11, and 15-16 Hz) were added absolutely and added to the SRSS of the remaining 26.

Justify the neglect of forcing frequencies above 31 Hz for

(a) torus shell loads, and

(b) submerged structure drag loads. (Arguments about small torus response do not apply for drag loads.) Why were CO drag loads (page 4-4) analyzed for 1-31 Hz only, but post-chug drag loads (page 4-5) for 1-50 Hz?

RESPONSE:

When the DBA CO load definitions were provided by the LDR, it soon became apparent that there were significant inherent conservatisms, not the least of which was the lack of any information about the phasing relationships between the Fourier harmonics. Clearly, conservatisms could have been maximized by applying all 50 CO harmonics using an absolute summation rule, and while some might infer this approach from the LDR and NUREG 0661, it was not prescribed. Various experts identified specific conservatisms and recommended approaches that would allow more realistic accounting for the potential DBA CO event. Some of the key findings by these experts follow:

From PUAR Reference 19 (or equivalently: GE/NEDE-24840), Section 3.4:

(1) The 5.5 Hz harmonic was the dominant content of the loading.

(2) "... all harmonics appear to be randomly phased relative to the dominant harmonic at 5.5 Hz."

(3) "... investigators have seen a tendency for a fixed phase relationship between the dominant harmonic and one or two multiples of the dominant (e.g., 5.5, 11, and 16.5 Hz) from examination of data from individual

pressure transducer records for the FSTF test, but showed random phasing for all other harmonics."

(4) While it was admitted that there appeared to be some relative periodicity of the harmonic amplitudes that would preclude the appropriateness of pure SRSS combination of the harmonic amplitudes, it was stated that "... it is highly improbable for more than about three harmonics to be worst-case phased at any one time..."

(5) "... a rule which requires about three harmonics to be absolute combined with all additional harmonics SRSS combined is consistent with the assumption of steady-state periodic amplitudes and random phasing."

(6) The LDR amplitudes are defined with significant conservatisms as can be seen from Figure 3-11 (especially in the frequency range from 40 to 50 Hz where most LDR amplitudes are much more than 100 percent greater than the average FSTF amplitudes).

(7) Also from Figure 3-11, it can be seen that actual FSTF amplitudes seem to show that CO has relatively little frequency content above 30 Hz.

From PUAR Reference 42, Section 4:

(8) Conclusion No. 2 states that: "For structures with frequency content similar to the FSTF or Oyster Creek torus and supports, only the harmonic responses below 30 Hz need to be computed and included."

Based on the findings listed and our own best technical judgment, TVA feels that neglect of the forcing frequencies above 30 Hz is justified for:

(a) torus shell loads

(b) submerged structure drag loads

An explanation of our reasoning follows:

As stated in finding (7), there is little frequency content of the CO loading above 30 Hz; this is the main reason for neglecting it. Additionally, for the BFN torus (even after substantial modifications that resulted directly from CO loads analysis), the responsive structural modes occur at frequencies below 30 Hz. Shapes of the higher frequency modes of the torus will not participate significantly with the shape of the CO pressure distribution. This argument

also applies for the post-chug loading on the torus since it has the same distribution shape as CO with only the harmonic amplitude coefficients being different.

For harmonic forcing components with frequencies more than 1.5 times the natural structural frequencies, the dynamic load factors (DLFs) become less than 1.0. For harmonic forces with frequencies greater than twice the natural structural frequencies, the DLFs are small and asymptotically approach zero. In this range, the forcing components would have negligible effect on the structure. This is the case with the torus for high frequency harmonics.

Further, empirical evidence of the adequacy of the BFN analytical approach for the DBA CO loading on the torus is provided in the responses to BNL item 7 (see Table BNL-7-1). Similar evidence is provided for the chugging loading on the torus in the response to FRC item 7 (see Table FRC-7-1).

Submerged structures are a different matter, however. Initially, most submerged structures were primarily responsive in the lower frequency ranges and were dominated by the DBA CO harmonics. In order to avoid highly amplified responses due to CO, pre-chug, and S/RV load definitions, virtually every submerged structure required substantial modification to stiffen and strenghten it. These modifications took some of the submerged structures into a responsive range with post-chug fluid drag. While it was impractical to stiffen submerged structures (most of them internal portions of large piping systems) above the post-chug forcing frequencies and still maintain viable designs for thermal loads, it was possible, after many iterations, to obtain designs that had sufficient strength to meet allowables for all load combinations. This left BFN with stiff submerged structures that were well within a range of post-chug drag, thus, necessitating use of the full 0 to 50 Hz range of the post-chug definition prescribed in the LDR. PUAR Plates 11, 18, 19, 20, and 21 show some of the stiffened submerged structures.

ITEM 7:

The approach of GE/NEDE 24840 - which is itself a departure from the LDR - calls for taking the sum of the four harmonics which produce the highest structural response, and adding them to the SRSS of the remaining harmonics. Were the forcing functions at 4-5, 5-6, 10-11, and 15-16 Hz the ones which produced the highest structural response for both torus shell and all drag loads? In the work done by SMA (References 19 and 42 of the BFN PUAR), the absolute summation of the four highest harmonics had nothing to do with phase relationships, but was an artifice used to arrive at an 84 percent nonexceedance probability (NEP). Based on the discussion in the PUAR, BFN's procedure does not guarantee an NEP of 84 percent. Justify BFN's departure from the recommended procedure and/or demonstrate structural margins which would adequately cover increases in the CO loads. Was Alternate 4 of the CO baseline rigid wall pressure spectrum applied to BFN?

RESPONSE:

While the approach recommended in PUAR Reference 19 (or GE/NEDE-24840) is a departure from the LDR, TVA believes it is well justified by the thorough studies and findings of many experts. Those findings clearly stress the extreme conservatism, hence inappropriateness, of absolute summation of all response harmonics.

As the approach is specified, it requires the identification of the three or four highest response harmonics of a structure to be combined absolutely with the SRSS of those remaining. This identification, however, is an impracticable task when one considers the number of structures to be analyzed and the response quantities of interest for each (e.g., displacement, acceleration, force, stress, stress intensities). Also, while this approach may guarantee 50 or 84 percent NEP for the CO loading alone, there can be no such claim for the controlling design load combinations involving CO since the points of maximum responses for CO load combinations are likely to be different than for CO alone. Therefore, TVA chose to vary slightly from the approach suggested in Section 6 of PUAR Reference 19. The approach used was justifiable and practical for timely, cost efficient implementation.

It cannot be guaranteed for both the torus shell and all submerged structures that forcing functions at 4-5, 5-6, 10-11, and 15-16 Hz were the ones producing the highest structural responses, although for some they may be--especially for the torus shell since its primary response

occurs around these frequencies. However, it is important to note that the suggestion to use the four highest response harmonics was an artifice to obtain an 84 percent NEP of an artificial load definition--one which Dr. Alan Bilanin has stated is 33 percent conservative just due to the presence of the bulkheads on the FSTF (see Reference BNL-7.1, Section 1, Equation 1.7).

There are the additional conservatisms of the LDR prescribed amplitudes, as already addressed by finding 6 listed in our response to BNL Item 6. And, specifically concerning torus shell responses, TVA has the conservatism of having applied a maximum envelope of the three LDR alternatives specified for harmonics between 4-16 Hz rather than selecting the <u>one</u> alternative producing maximum response.

To pursue the issue of why TVA chose forcing functions at 4-5, 5-6, 10-11, and 15-16 Hz, the following arguments are offered:

(1) As contended, it is a practical impossibility to identify the three or four highest CO response harmonics for all structures and response quantities. Therefore, TVA sought a practical alternative that would maintain some conservatism over a pure SRSS combination of the CO harmonics. Because of the reported indications that there may be some fixed phase relationship between the dominant harmonic at 5.5 Hz and its first few multiples, we decided to use the 5-6, 10-11, and 15-16 Hz LDR harmonics. The 4-5 Hz harmonic was added to this list since it was the next largest amplitude harmonic in the LDR definition. It should be noted that three of these (4-5, 5-6, and 10-11 Hz) are the highest of all the amplitudes provided in the LDR.

(2) Comparing the LDR prescribed DBA CO and post-chug amplitudes, it can be seen that for structures having primary response modes below about 20 Hz, CO load combinations would be expected to control for design since the CO amplitudes below 20 Hz are generally larger than the post-chug amplitudes. Structures having primary response modes above 20 Hz would most likely be controlled for design by post-chug load combinations since post-chug amplitudes are higher in this range. Therefore, by picking three of the highest CO amplitudes for absolute summation, the three potentially most damaging load components are assured of receiving conservative combination in the response predictions for structures likely to be controlled in their design by CO load combinations.

(3) PUAR Reference 19 recommends a procedure for obtaining 50 percent or 84 percent NEPs and shows that this is achieved when the three or four highest response harmonics are combined absolutely. This is based on comparisons with predicted response values at these probabilities as taken from constructed CDF curves for both the FSTF and Oyster Creek torus. As can be seen from the CDF curves of Figures 4-6 through 4-10 from Reference 19, all have relatively small variance as indicated by their steep slope. It can also be seen that the response values predicted by total absolute sum of all harmonics is well above the response value associated with 100 percent NEP. Therefore, while even a total SRSS combination of all harmonics would be only slightly unconservative relative to the CDF 50 percent and 84 percent NEP response values, a total absolute combination would be grossly overconservative.

(4) While there is no reason to suspect that a total SRSS combination of all harmonic responses would produce a response value as low even as that associated with a 0 percent NEP, it is interesting to observe from PUAR Reference 19, Figures 4-6, 4-7, 4-8, 4-9, and 4-10, that the percentage differences between the 0 and 50 percent NEP response values are 11.3, 15.6, 16.3, 24.0, and 18.2 percent, respectively. Therefore, even a pure SRSS combination rule would result in at least a 0 percent NEP response value, meaning the potential unconservatism could be no more than the above percentage differences between 0 and 50 percent NEP values. Further, since TVA's approach is more conservative than pure SRSS, our predicted response values would be still less of a percentage difference. All of these arguments mean that any slight unconservatism there may be in TVA's approach is much more than offset by the inherent conservatism in the FSTF based load definitions. Inherent in those definitions, as already mentioned, is at least a 33 percent conservatism according to Dr. Alan Bilanin.

So, while our approach does not rigorously assure 84 percent NEP of the conservative LDR load definitions per se, we feel very confident that this level or more would be achieved if more realistic load definition and analysis techniques were possible. A strong indication of the conservatism of the BFN DBA CO analysis is seen in the attached Table BNL-7-1. BFN stresses and reaction forces are presented, factored as nearly as possible to an FSTF-equivalent basis, and compared to measured and calculated NEP values for the FSTF.

Looking at Table BNL-7-1, the factored BFN cradle support pad reaction forces are seen to be conservative with respect to the 84 percent NEP values (this would indicate similar conservatism of the stresses in the critical cradle regions which required extensive modifications). Also, the BFN BDC membrane stress intensity (factored to an FSTF-equivalent basis) is almost exactly the same as the 84 percent NEP value for the FSTF. While this degree of closeness may be coincidental, it does provide additional evidence that there is no large deficiency in stress intensity predictions in the BFN analysis.

Finally, there are two additional conservatisms worth noting about the BFN analytical approach. First, 2 percent damping was used for the DBA plus S/RV load combination analyses of the torus and submerged structures even though higher damping is justifiable because of the higher service level allowables. Second, conservative load combination techniques were applied (see PUAR Section 4.4.2).

Concerning the final question about Alternate 4 of the CO baseline rigid wall pressure spectrum, we do not know to what this refers.

Additional Reference:

BNL-7.1 Structural Mechanics Associates, "A Statistical Basis for Load Factors Appropriate for Use with CO Harmonic Response Combination Design Rules," Report No. SMA 12101.04-R003D, March 1982.

Addendum

In the September 5, 1984 meeting, BNL expressed remaining concerns over TVA's use of the absolute sum of the four highest DBA CO harmonic amplitudes, rather than the four harmonics causing the greatest response. BNL also asked: "How much greater could the DBA CO load be without exceeding allowables"? (paraphrased)

Our response considers the torus separately from the tiedown system for reasons which are explained below.

The most highly stressed regions of the torus, relative to allowables, are in the cradle adjacent to the scab plates described in PUAR Section 5.2.4.3. (Also see the response to FRC Item 11.) The controlling load combination is number 14 which does not include DBA CO. There are large margins

for all load combinations involving DBA CO. If one assumes that cradle stresses are directly proportional to the net compressive loads, the DBA CO reactions could be 2.5 times the values computed by the TVA analysis without exceeding allowables.

The tiedown system, on the other hand, is controlled by load combination number 27 which includes DBA CO. Tiedown stresses are directly proportional to net uplift loads. From computer calculated responses to the 0 to 30 Hz unit amplitude harmonics and hand calculations, the increase in reactions by taking the four highest responses, rather than the responses to the four highest amplitudes, has been quantified. The conservatism of TVA's method of enveloping the three alternate sets of amplitudes has also been quantified. These calculations show that the DBA CO reactions presented in Table BNL-7-1 would be 9 percent higher if the four highest harmonic responses had been used, while retaining the conservatism of enveloping the alternate amplitudes. If the individual alternate amplitude sets are used, the reactions would be 5.4 percent higher than those in the table.

With the 5.4 percent increase, the tiedown system stresses do not exceed allowables. It is important to reemphasize that the SMA method of Reference 19 provides large margins for support reactions. It is also noteworthy that the limiting load combination (number 27) includes the highly unlikely simultaneous occurrence of the maximum responses due to the safe shutdown earthquake, DBA CO, and a single valve S/RV actuation. TVA combined these three dynamic events absolutely. If, for example, a 1.1 SRSS combination of the three dynamic loads had been used, the uplift loads would have been barely great enough to overcome the deadweight.

TABLE BNL-7-1

COMPARISON OF FSTF AND BROWNS FERRY DBA C.O. RESPONSES

RESPONSE QUANTITY	BFN CALCULATED RESULTS	BFN RESPONSES FACTORED TO EQUIVALENT FSTF	MEASURED FSTF, PER REF.19 TABLE 7-2	50% NEP FSTF, PER REF.19 TABLE 6-2	84% NEP FSTF, PER REF.19 TABLE 6-2
BDC MEMBRANE STRESS INTENSITY (KSI)	1.98	2.77[1]	2.6	2.47	2.79
INSIDE REACTION (KIPS)	306	202[2]	93	122	140
OUTSIDE REACTION (KIPS)	333	220[2]	110	140	159

(1) FSTF EQUIVALENT SHELL S.I. = $S_{BFN}\left[\frac{(R/T)FSTF}{(R/T)BFN}\right]\left[\frac{1}{\text{PLANT UNIQUE PRESSURE FACTOR}=0.85}\right] = 1.40 S_{BFN}$

WHERE, R = MINOR RADIUS OF THE TORUS, T = SHELL THICKNESS, AND S = STRESS INTENSITY

(2) FSTF EQUIVALENT SUPPORT REACTIONS = (BFN REACTION) $\left(\frac{\text{FSTF POOL AREA PER COLUMN PAIR}}{\text{BFN POOL AREA PER CRADLE}}\right)$ X

$\left(\frac{1}{\text{PLANT UNIQUE PRESSURE FACTOR}}\right) = 0.661$ (BFN REACTION)

ITEM 8:

Were pre-chug loads applied to BFN according to the LDR and NUREG 0661 specifications regarding amplitude, circumferential and vertical distribution and cycle duration? If not, provide quantitative justification.

RESPONSE:

The pre-chug loads were applied in complete accordance with the LDR and NUREG 0661, including considerations of amplitude, circumferential and vertical distribution, and cycle duration. With regard to the latter, the responses of 71 shell modes due to six independent harmonic (implying infinite duration) forcing functions, fine-tuned to the structural frequencies, were enveloped for all points in the model. No credit was taken for the finite duration of the actual event.

ITEM 9:

For post-chug loads, were the harmonic forcing functions used in the 1-30 Hz range the ones specified in the LDR, and were they applied in the manner prescribed in the LDR? If not, justify departures.

RESPONSE:

For both the post-chug pressure loads applied to the torus and the drag loads applied to internal structures, the harmonic forcing functions used in the 1-30 Hz range were those specified in the LDR, and they were applied in the manner prescribed by the LDR. Appendix D, Section D.1.2.4.2 of the BFN PUAR explains how the LDR prescribed method was applied for submerged structures by considering the closest downcomer load sources together with worst-case phasing between the sources.

ITEM 10:

The finite element model of Figure 6-7 shows amputated downcomers. How were the CO and CH loads applied to these amputated downcomers?

RESPONSE:

The finite element model in Figure 6-7 was used to examine more closely the vent downcomer/header intersection. Loads for the different combination events which included condensation oscillation and chugging were extracted from the 45° vent system beam model (PUAR Figure 6-2) at the node representing the downcomer/vent header shell intersection. These loads were then input into the truncated model at the end of the downcomer. (The downcomer end is comprised of rigid beams connected by a node in the center.) The appropriate stresses were then extracted and compared to the stress allowables.

ITEM 11:

Were the CO loads applied to the downcomers in accordance with the LDR and NUREG 0661? Were the eight load cases of Section 4.4.3.2 of the LDR analyzed for all relevant vent system parts (including main vent/vent header intersection, drywell/main vent interaction, downcomer/vent header intersection, etc.)? The PUAR explicitly mentions considering different load cases only for the downcomer/tiebar intersection, and in that case refers only to four load cases rather than the eight of the LDR (Section 6.7.1.2.1). Why is 2.5 percent damping justified for BFN for CO lateral load analysis?

Note that Table 6-10 shows no margin for the downcomer/vent header intersection in Load Combination 27 which involves CO.

RESPONSE:

The CO downcomer loads were applied in a manner consistent with the intent of the LDR and NUREG 0661. The load from the differential pressure for one downcomer was added to the internal pressure, that occurs simultaneously in all downcomers, thereby producing a higher load in one downcomer in each pair. Thus, from Figure 4.4.3.4 of the LDR, a darkened downcomer indicated that the differential and internal pressures were working together simultaneously, whereas the other downcomer in the pair experienced only the internal pressure.

Based on the primary downcomer swing frequency extracted from a modal analysis of the system, sinusoidal forcing functions were applied to downcomer pairs defined by Figure 4.4.3-3 in the LDR. Since the primary swing mode for the BFN system occurs at approximately 8 Hz, the 1st, 2nd, and 3rd harmonics were applied in the 4, 8, and 12 Hz ranges, respectively.

Another aspect of the BFN analysis was the application of the first harmonic forces to the coincident 8-Hz swing frequency. Response of the system to this single frequency load envelops the sum of the three harmonics defined by the LDR. This load was subsequently applied in the stress evaluation. Also, the first harmonic force amplitudes were applied with 16 and 24 Hz sinusoidal functions to verify that higher frequency responses do not impact the total CO response. In actuality, 30 individual sinusoidal functions were applied for each load case to account for potential response at the 1/2, 1, 1-1/2, 2, and 2-1/2 harmonics of the six discreet primary swing mode frequencies in the 8-9 Hz range. Note that this load was in addition to the vent system CO loads which were applied in a separate analysis.

Four load cases were initially analyzed for downcomer CO lateral loads as indicated by PUAR Figure 6-12. From inspection of the first four load cases and resulting stresses, it was evident that in each instance, the worst effect on a downcomer would occur on one that was located on the inboard side of the vent header. Furthermore, the highest loaded downcomer (unreinforced shell) resulted from the application of Load Case 1 (differential pressure applied to all inboard downcomers). Since the second four load cases defined in revision 2 of the LDR are mirror images of the first four cases and greater response resulted from Case 1, it was resolved that the worst loading had already been analyzed. Therefore, no further analysis was performed.

All critical locations of the vent system were evaluated for DBA CO lateral load combinations. As noted in item 11, the stress margin relative to Service Level B allowables for the CO combination in Table 6-10 of the PUAR is close to 1.0 for the primary plus secondary stress category. This stress level should be evaluated with consideration of the conservatism in the load combination (event 21 is a Service Level C combination) and the fact that downcomer lateral Load Case 1 is the worst of the eight potential load configurations.

Preliminary analysis of the BFN containment vent system for the DBA CO lateral load definition indicated a surface stress level in the vent header shell near the downcomer that approached the yield stress value for SA-516 Grade 70 steel. Under this situation the total stress level for load combination No. 21 would not meet the allowable for primary plus secondary stress range. In an effort to avoid additional modification (i.e., downcomer/vent header reinforcement gussets), the 2 percent recommended damping ratio was investigated as a source of excessive conservatism. Per Regulatory Guide 1.61, a 3 percent damping value is recommended for analysis of large diameter piping systems for the safe shutdown earthquake. Furthermore, the calculated damping value resulting from the snap pull test of a tied downcomer arrangement (see Figure 4-5 in Reference 5 to supplement 1 of NUREG 0661) was found to be approximately 2.2 percent for a 50 percent yield. Also, the damping versus strain curve indicates a rapid increase in damping above the 50 percent yield level. Based on these findings, it was concluded that a damping value greater than 2 percent but less than 3 percent is appropriate for the Browns Ferry configuration. The 2.5 percent value was selected as the midpoint of the 2-3 percent range and utilized for the DBA CO downcomer lateral analysis. Resulting surface stresses in

the vent header shell at the downcomer intersection are 20 to 24 ksi (for DBA CO loading alone) as compared to a yield stress value of 32.6 ksi for SA-516 Grade 70 steel at 400°F.

Therefore, the 2.5 percent damping value is justified based on:

(1) The structural response of the Browns Ferry downcomer/ vent header configuration.

(2) The projected results of the snap test for higher initial stress levels.

(3) The damping criteria delineated in Regulatory Guide 1.61.

ITEM 12:

Were the chugging loads applied to the downcomers in accordance with the LDR and NUREG 0661? Were the multivent chugging loads accounted for on all vent system parts in accordance with the LDR and NUREG 0661?

Note that according to Table 6-10, Load Combination 15, which involves CH, has relatively little margin.

RESPONSE:

Yes, the chugging loads were applied to the vent system in accordance with the LDR and NUREG 0661. LOCA chugging loads included post-chug drag, chugging lateral, acoustic vent system pressure oscillation, and gross vent system pressure oscillation, which were applied to the beam models shown in PUAR Figures 6-2 and 6-3. Responses were determined from those models and local stresses were calculated for the critical locations.

ITEM 13:

What hydrodynamic load definition was used for the vent pipe drain referred to on page 6-10 and shown on Figure 6-8?

RESPONSE:

From a Stardyne model of the vent drain and support system, the fundamental natural frequency of the system was found to be 35.1 Hz. Clearly, high amplitude harmonics of post-chug around this frequency would lead to a strong expectation that a load combination involving post-chug would be controlling; although, the possibility of a combination with pool swell was also considered. From investigations of all potentially controlling design load combinations (including associated service level allowables) it was determined that combination 11 (see Figure 4.3-1 of NUREG 0661) was controlling. Specifically, the design case determined to be controlling was the SBA combination of S/RV plus post-chug fluid drag loads under service level A allowables.

The dynamic loads were very conservatively accounted for by the "Equivalent Static Load Method" explained in Appendix D, Section D.1.2.2 of the BFN PUAR report. All 50 post-chug bubble source amplitudes and FSI acceleration coefficients were summed and used as multipliers of the unit forces $(F_{or})_{BUB}$ and $(F_{or})_{FSI}$ described in Equations D.1.2-6 and D.1.2-8, respectively. To these a resonant DLF = 25 (assuming 2 percent damping) was conservatively applied. The S/RV load contributions were applied with a harmonic DLF = 1.2 based on the ratio of maximum S/RV bubble frequency-to-system frequency of 14.7/35.1 (again assuming 2 percent damping).

Addendum

In the September 5, 1984 meeting, BNL's consultant, Professor Sonin of MIT, asked if the potential for chugging through the vent drain pipe and the effects of the resulting lateral loads had been considered.

TVA responded that the LDR did not include a method for defining such loads, and the effects could therefore not be evaluated. Professor Sonin then asked to be provided the properties and dimensions of the drain pipe and its support and the drag loads which had been applied to them.

A set of five pages of calculations on the effects of S/RV and post-chug drag loads were subsequently transmitted to Professor Sonin through NRC. The calculations show the post-chug drag loads, particularly, were defined in an extremely conservative manner which should compensate for the lack of a directly applied lateral chugging load.

ITEM 14:

Combining individual S/RV shell pressures by SRSS to obtain multiple valve shell pressures is an exception to the AC. Justify this procedure for BFN.

RESPONSE:

The use of SRSS to obtain multiple valve shell pressures for analysis of S/RV discharges is justified by the BFN plant unique S/RV tests (PUAR Reference 41) and the correlation of analysis and test results (PUAR Appendix C).

Section C.3.2 of the PUAR specifically addresses this issue. The measured peak shell pressures during multiple valve tests were approximately 45 percent of the analysis values for single valve tests and 54 percent of the analysis values for multiple valve tests. Thus the multiple valve test pressures are correlated by a 1.2 SRSS of single valve test pressures, but the overall BFN analysis and design approach was clearly conservative.

It is also noteworthy that considerable care was taken in the BFN test to ensure simultaneous actuation of three S/RVs with adjacent discharge locations in the torus. This represents a "worst location" in the torus. Referring to PUAR Figure 7-3, S/RVs D, E, and M were actuated simultaneously for multiple valve tests. S/RV E was actuated for single valve tests. Excellent repeatability was demonstrated for both test series (five single valve tests and four multiple valve tests.)

ITEM 15:

Clarify the statement that the torus was analyzed quasi-statically for S/RV hydrodynamic shell pressures. Where does g(t), i.e., the wave form of the pressure history, in the expression on page 5-13 of the PUAR come from? Are pressures applied statically as stated on page 5-12 or is there a time variation as implied by the expression on page 5-13?

RESPONSE:

The wave form of the pressure history, g(t), was generated by the QBUBS02 computer code. The pressures were applied statically to the torus shell to determine torus stresses, deflections, and support loads. Subsystems, such as attached piping, were analyzed dynamically for the acceleration response resulting from the assumed shell motion (see page 5-14 of the PUAR).

ITEM 16:

Provide the following additional information regarding the in-plant S/RV tests conducted at BFN and the S/RV design loads extrapolated from the tests:

1.0 Description of the tested Quencher Device -

1.1 Drawings showing details of the quencher geometry - plan, elevation, arm length, arm diameter, hole arrangement, spacing, size, etc.

1.2 Location of quencher device relative to suppression pool boundaries and suppression pool surface.

1.3 Any difference between the tested quencher configuration and the Monticello version (as described in GE/NEDE-24542-P) highlighted and quantified.

2.0 A description of the loads observed during testing -

2.1 Peak overpressure (POP) and underpressure (PUP) recorded on the torus shell during each relevant S/RV actuation.

2.2 A measure of the frequency content of each pressure signature.

3.0 A description of the test conditions -

3.1 Geometry of the tested SRVDL (diameter, length, free volume, and routing below pool surface).

3.2 Geometry of any SRVDLs in the plant that differ significantly from the tested SRVDL.

3.3 S/RV steam flow rate (MS), pool temperature (TPL), pipe temperature (TP), water leg length (LW) and pressure differential (ΔP), if any, for each test.

3.4 Minimum ΔP permitted by NRC Technical Specification and corresponding LW for all SRVDLs.

4.0 A description of the design conditions for each load case used for design -

4.1 Geometry of all SRVDLs involved and their azimuthal location in the torus.

4.2 TP, TPL, MS, ΔP, and LW for all SRVDLS involved.

5.0 A description of the design loads for each load case -

5.1 Normalized pressure signature.

5.2 Single valve POP/PUP values.

5.3 Spatial attenuation of the POP/PUP values (if this differs from the LDR methodology, sufficient additional torus shell pressure data must be supplied to justify such deviation).

5.4 Frequency range considered.

RESPONSE:

1.0 Description of the tested quencher device -

1.1 The plan view of all BFN quenchers in Units 1 and 2 is shown on TVA drawing 47W401-7. For Unit 3 the plan view is shown on drawing 47W401-3. The tested quenchers were in Unit 2 at azimuths 78°-45' (D), 101°-15' (E), and 123°-45' (M). S/RV E was actuated for single valve tests and all three (D, E, and M) were actuated for multiple valve tests. These plan views correspond to PUAR Figure 7-3.

BFN quencher arm details are shown on TVA drawing 47W401-5. All BFN quenchers are identical in design.

Copies of all referenced drawings are available for review.

1.2 The BFN quencher device locations are shown on TVA drawings 47W401-3, 47W401-5, and 47W401-7. Each quencher centerline is at elevation 526.5 which is 5.0 feet above the bottom of the torus shell. This yields a submergence of approximately 10.0 feet. Typical BFN quencher installations are shown on PUAR plates 10, 11, and 13.

1.3 The BFN quencher device utilizes the previously existing 10-inch ramshead as indicated on drawing 47W401-5, while the Monticello version has a 12-inch ramshead. The BFN device has a 10-inch x 12-inch reducer between the ramshead and quencher arm while the Monticello version does not. BFN and Monticello quencher arm designs are identical

except for minor variations in support type and location. The BFN weld cap hole pattern matches the pattern shown in Figure 1-2 of NEDE-24542-P; it does not match the pattern in Figure 1-3 of that report.

2.0 A description of the loads observed during testing -

2.1 Torus shell pressures resulting from the S/RV test are discussed in Appendix C, Paragraph C.5.2 of the PUAR. Table C-2 of the PUAR presents a comparison of the analytically predicted pressures versus the average of the peak pressures from each test. This information is from the TES Report No. 5172 (PUAR Reference 41). Pages 1 through 54 of Volume III of the TES report show the pressure traces of the torus shell for each test. A summary of the maximum and minimum pressures (POP and PUP) recorded during each test are shown in Tables BNL-16-1 and BNL-16-2.

2.2 The pressure traces for all locations and each test are found in the TES Report (PUAR Reference 41). All pressure traces are similar in shape and primary frequency. The primary frequency of the pressure traces ranges from 5.5 to 6.5 Hz. Typical pressure traces are shown in Figure BNL-16-1.

3.0 A description of the test conditions -

3.1 & 3.2 The geometry of all SRVDLs is shown on the TVA 47W401 drawing series. All discharge lines are 10" SCH 40 in the drywell and 10" SCH 80 or 10" SCH 60 in the wetwell. The routing for all lines below the pool is the same. The routing in the torus above the pool can be grouped into two categories--long lines and short lines. SRVDL E, a long line, was chosen for the single valve tests since the long line should represent the worst case for S/RV blowdown. S/RVs D, E, and M were actuated simultaneously for the multiple valve tests. The initial gas volume for all lines is shown in Table BNL-16-3. Also, see 1.1 above.

3.3 Test Conditions

	Line D	Line E	Line M
MS, lb/sec	268	268	268
TPL, °F	78-81	78-81	78-81
TP*, °F	238-355	220-379	246-361
LW, FT	7.0	7.0	7.0
Δ P, psid	1.2-1.33	1.2-1.33	1.2-1.33

*Initial and final temperatures of drywell pipe gauge.

3.4 The minimum ΔP permitted by technical specifications is 1.10 psid. The corresponding water leg length is approximately 7.5 feet measured from the quencher centerline elevation.

4.0 A description of the design conditions for each load case used for design -

4.1 Figure 7.3 of the PUAR shows a plan view of the S/RV discharge in the torus. This information as well as other information regarding geometry is available from TVA drawing series 47W401. Also, see 1.1 above.

4.2 The following parameters were extracted from selected RVR1Z, RVFOR input.

Case A1.1 (NOC)

SRVDL	TP, °F	TPL, °F	MS, lb/sec	ΔP, psid	LW, ft
E	115	75	308	1.2*	7.13
L	115	75	308	1.2*	7.13

Case C3.3 (IBA with Steam in DW, Second Actuation)

SRVDL	TP, °F	TPL, °F	MS, lb/sec	ΔP, psid	LW, ft
E	350	90	308	1.0*	40.12
L	350	90	308	1.0*	31.56

*These values were used in RVR1Z, a value of zero was used for RVFOR.

5.0 A description of the design loads for each load case -

5.1 Normalized pressure signature -

We interpret the term "normalized pressure signature" to mean the variation of the shell pressures with time. Therefore, it is the same as the variable g(t) defined in Section 5.4.2.8 of the PUAR, and generated in accordance with the LDR by GE computer code QBUBS02. Also, see the response to BNL Item 15.

5.2 The largest magnitude POP and PUP values generated by QBUBS02 were applied for each SRVDL in the torus. Per the LDR, first actuation pressures were conservatively assumed to be possible for second actuation (reflood) conditions. The single valve values are as follows:

	Pressure (psig)	
Event	POP	PUP
NOC or DBA	16.2	11.9
SBA or IBA	19.7	16.6

5.3 The spatial attenuation functions used were as defined in the LDR and generated by QBUBS02. The only deviation from the LDR in this regard was the use of SRSS for combining the effects of multiple valve actuations. The SRSS issue is addressed by the response to BNL Item 14.

5.4 The frequency range used for design, as provided by Section 5.5.2 of the PUAR, is as follows:

	Frequency (Hz)	
Event	Minimum	Maximum
NOC or DBA	4.16	10.29
SBA or IBA	5.58	14.69

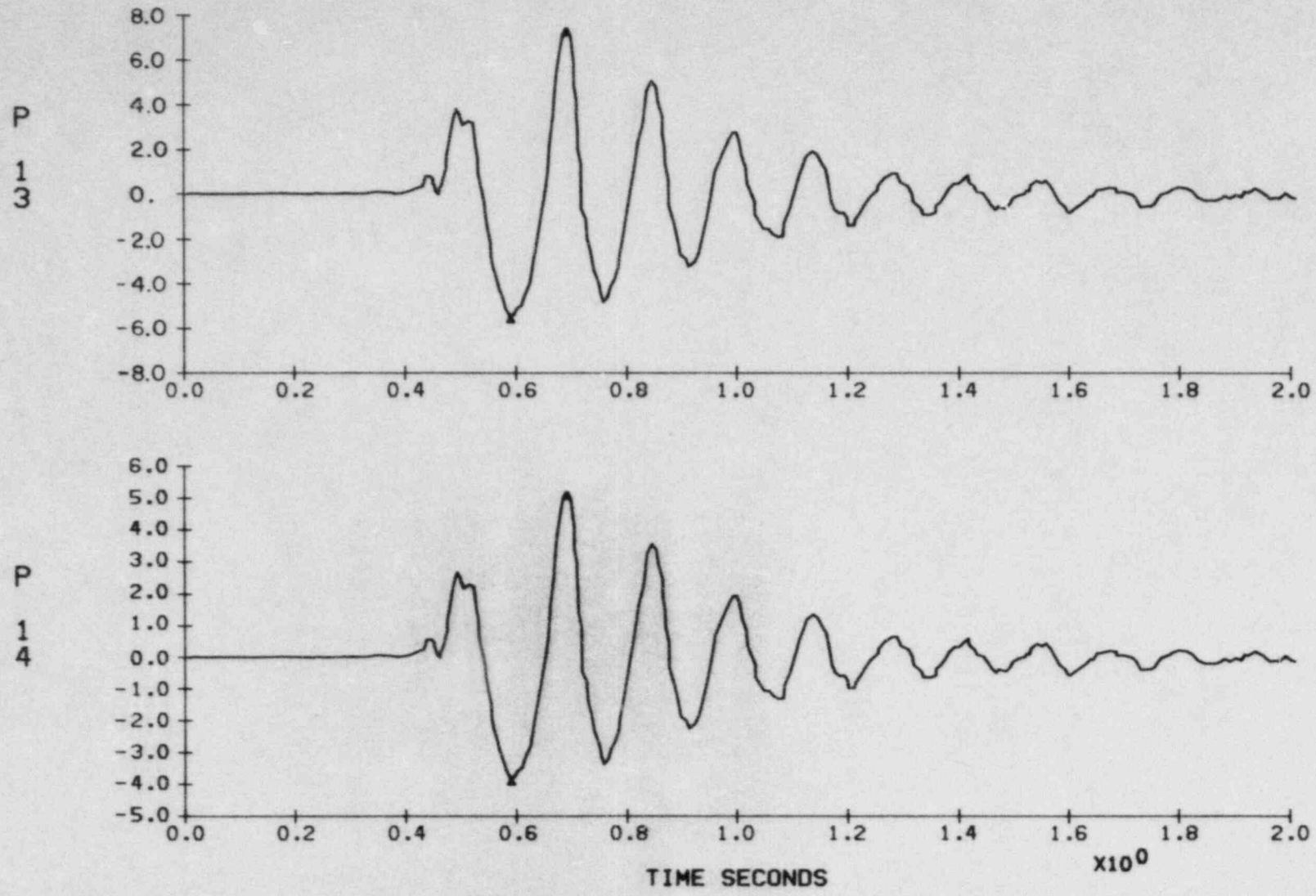

FIGURE BNL-16-1

TYPICAL PRESSURE TRACES FOR BFN TORUS SHELL

TABLE BNL-16-1
MAXIMUM AND MINIMUM PRESSURES (PSI)

SINGLE VALVE ACTUATION TESTS

LOCATION	S1	S2	S3	S4	S5
1	5.648	6.417	6.714	6.695	5.971
	-4.950	-5.596	-5.538	-5.545	-5.293
2	5.870	6.743	7.233	7.112	6.232
	-5.203	-5.898	-5.827	-5.849	-5.529
3	5.393	6.455	6.979	6.550	5.800
	-4.825	-5.386	-5.451	-5.429	-4.949
4	4.593	5.285	6.004	5.709	5.183
	-3.950	-4.477	-4.650	-4.509	-4.195
7	3.105	4.077	5.297	4.620	4.151
	-2.354	-4.097	-4.258	-3.929	-3.467
8	5.195	5.746	5.501	5.814	5.113
	-3.554	-3.990	-3.969	-4.112	-3.915
9	1.757	1.670	1.878	1.810	1.650
	-1.113	-1.482	-1.341	-1.354	-1.341
10	2.539	2.737	2.621	2.751	2.512
	-1.716	-1.988	-1.961	-2.008	-1.900
12	2.226	2.369	2.580	3.057	2.764
	-1.648	-1.859	-2.036	-1.838	-1.634
13	6.158	6.996	6.757	6.919	7.046
	-4.755	-5.397	-5.249	-5.333	-5.383
14	4.887	5.615	5.517	5.496	5.461
	-3.655	-3.907	-3.732	-3.858	-3.970

TABLE BNL-16-2
MAXIMUM AND MINIMUM PRESSURES (PSI)

MULTIPLE VALVE ACTUATION TESTS

LOCATION	M1	M2	M3	M4
1	4.685	6.029	8.123	7.005
	-5.997	-6.062	-6.333	-6.359
2	6.211	7.283	9.135	8.617
	-6.310	-6.438	-6.771	-6.786
3	7.787	8.857	9.956	10.00
	-6.150	-6.434	-6.688	-6.66
4	9.204	10.01	10.79	10.66
	-6.016	-6.485	-6.760	-6.491
7	6.471	6.310	8.523	6.216
	-4.922	-4.613	-5.659	-5.686
8	5.828	6.795	8.224	8.007
	-4.623	-5.174	-5.331	-5.590
9	1.348	1.764	2.642	2.903
	-1.831	-1.777	-1.837	-1.509
10	2.151	2.669	3.288	2.914
	-2.192	-2.185	-2.383	-2.240
12	11.98	11.00	10.36	11.16
	-7.482	-7.639	-7.162	-7.196
13	7.616	8.328	7.919	7.264
	-6.108	-5.876	-6.524	-5.953
14	5.314	6.140	6.343	5.076
	-5.300	-5.356	-5.097	-4.579

TABLE BNL-16-3

LINE	INITIAL GAS VOLUME (FT^3) A1.1 NORMAL OPERATING CONDITION BLOWDOWN	
D	73.80	
H	75.37	LONG LINES
E	66.16	
A	58.31	
F	53.33	
L	55.07	
G	52.14	
K	54.82	SHORT LINES
B	51.00	
C	52.69	
J	55.60	
N	54.82	
M	54.93	

ITEM 18:

What is the vertical location of the suppression pool temperature sensors in relation to the S/RV T/Quencher centerline?

RESPONSE:

The sensors are located approximately 20 inches above the T-Quencher centerline and at mid-bay. (See PUAR Figure 10-7.)

ITEM 19:

Were there any exceptions to the AC for the hydrodynamic loads applied for analysis of the Torus Attached Piping? If so, elaborate.

RESPONSE:

Other than the general interpretations elaborated in Section 4.2 of the BFN PUAR, there were no specific exceptions to the NUREG 0661 AC for the hydrodynamic loads applied for analysis of the torus attached piping.

ITEM 20:

In the calculation of various drag loads for BFN, the computer codes LOCAFOR, CONDFOR, TQFORBF, and TQFORO3 were used. Do the algorithms of these codes follow approved AC procedures? State any exceptions and justify them.

RESPONSE:

The GE computer codes LOCAFOR, CONDFOR, TQFORBF, and TQFORO3 were used in the calculation of various drag loads for BFN. These codes were put up on Control Data Corporation computers around the country for access by the different AEs performing Mark I plant unique long-term program evaluations. These codes were developed, documented, and verified by consultants under contract with GE, not by the AEs performing the Mark I analyses. The codes are proprietary to GE and were only provided as "black boxes" with instructions on their use (including description of required input data) provided in the form of Application Guides. The AEs (including TVA) therefore do not have the direct access to the specific algorithms of these codes which would be necessary to answer your question definitively. It is TVA's understanding, however, that the codes LOCAFOR, CONDFOR, and TEEQFOR, used for evaluation of pool swell, CO and chugging, and S/RV drag loads, respectively, follow approved NUREG 0661 AC procedures. That means that TVA has defined only S/RV drag loads with codes not thought to specifically follow all NRC-approved AC procedures.

The only significant differences between the approved code TEEQFOR (not used by TVA) and the TQFORBF and TQFOR03 codes, to TVA's knowledge, are as follows:

TQFORBF - This code is different in that two bubble pressure factors, BFAC(1) and BFAC(2), were incorporated to be used as multipliers of the negative and positive bubble pressures, respectively. These were empirically developed factors used to obtain more realistic comparisons of code predictions to Monticello test results (see Appendix B of GE Application Guide 5, Revision 3 - a later revision of PUAR Reference 63).

TQFOR03 - This code is different in the bubble dynamics portion of the code which uses QBUBS03 instead of QBUBS02. The result is that far more realistic load predictions are obtained from this code due

to the attenuation in bubble energy as it rises to the surface of the torus pool. Particularly for structures located high in the pool, this code predicts drag loads that are significantly attenuated in amplitude with time.

While both of these codes are felt to be more realistic than the extremely conservative TEEQFOR code, it should be noted that the least conservative code, TQFOR03, was only used for the downcomer S/RV drag load predictions. That was because the downcomers are located very high in the pool where, realistically, the S/RV bubbles have attenuated substantially from their exit strength. Loads predicted for this structure using even the TQFORBF code (which is slightly less conservative than TEEQFOR) were found to be unrealistically high.

For all submerged structures other than the downcomers, the still very conservative TQFORBF code was used to obtain peak S/RV drag force amplitudes. This code was used for the other submerged structures because it is cheaper to run than TQFOR03 and the degree of overconservatism in TQFORBF versus TQFOR03 is not too significant for structures in lower elevations of the pool. Other than the downcomers, most BFN submerged structures are in the lower pool elevations.

The use of TQFORBF and TQFOR03 was believed to be well justified by good engineering judgment and especially by the fact that TVA planned S/RV tests which were expected to support that judgment. Additionally, the S/RV drag (except for the downcomers) were conservatively defined assuming worst-case peak load amplitudes, applied as steady-state harmonics at worst-case frequencies.

As expected, the S/RV tests provided conclusive evidence of the adequacy of the analytical appraoch for S/RV fluid drag loads. Appendix C of the PUAR describes the correlation of analytical and test data. For example, the analytical approach for the downcomers (using TQFOR03 loads) was shown to overpredict stresses by a factor of four relative to single and multiple S/RV test results.

ITEM 21:

Are there any differences between Browns Ferry Units 1, 2, and 3 which were significant enough to warrant separate analyses for any unit? If so, state the differences and the analyses used.

RESPONSE:

Torus

The Units 1 and 2 tori are virtually identical. Unit 3 used lighter construction in the following areas:

Location	Units 1 and 2	Unit 3
Ring girder inside flange	1-1/2" x 12"	1" x 10"
Ring girder web	1-1/4" x 12"	3/4" x 12"
Cradle edge plates	1-1/4" 12"	1" x 12"

All dynamic torus analyses and the definition of modifications were based on the Unit 3 properties. Modification studies showed that stiffening the ring girder-cradle system always improved performance. Hence, the definition of modification for Units 1 and 2 from the Unit 3 analysis results is conservative.

Vent System

The vent systems for all BFN units are virtually identical.

Torus Attached Piping

External BFN torus attached piping configurations are different for each BFN unit. Therefore, generally a separate piping analysis was required for every piping system on each unit.

Internal torus attached piping configurations are virtually identical from unit to unit but they are included in the external piping analytical models.

S/RV Discharge Piping

Two basic S/RV piping configurations are used in each BFN torus as shown by PUAR Figures 7-8 and 7-9. The arrangement of all 13 lines in each BFN torus is shown in plan view by PUAR Figure 7-3. BFN S/RV drywell piping configurations vary from line to line and and in some cases unit to unit. Therefore, various analytical models were used for the S/RV piping in the drywells.

Nonsafety-Related Internal Structures

The nonsafety-related internal structures are virtually identical for all BFN units.

ITEM 22:

This is an additional item to respond to a verbal inquiry from BNL at the September 5, 1984 meeting. BNL asked how close to impact with the main vent bellows does the pool swell come.

RESPONSE:

Calculations, based on the conservative LDR methodology, predict that the pool swell profile would come within 1.1 inches of the bellows at the closest point. If the pool swell were to slightly impact the bellows, the velocity would be very small, approaching zero at incipient impact.

Examination of the construction of the bellows leads to the assessment that it has very good local impact resistance. Any potential for damage or leakage would require impact over a large area, which, in turn, would require the pool to rise at least a foot or more above the bottom of the bellows.

TVA concludes that there is no significant safety concern for pool swell impact on the vent system bellows.

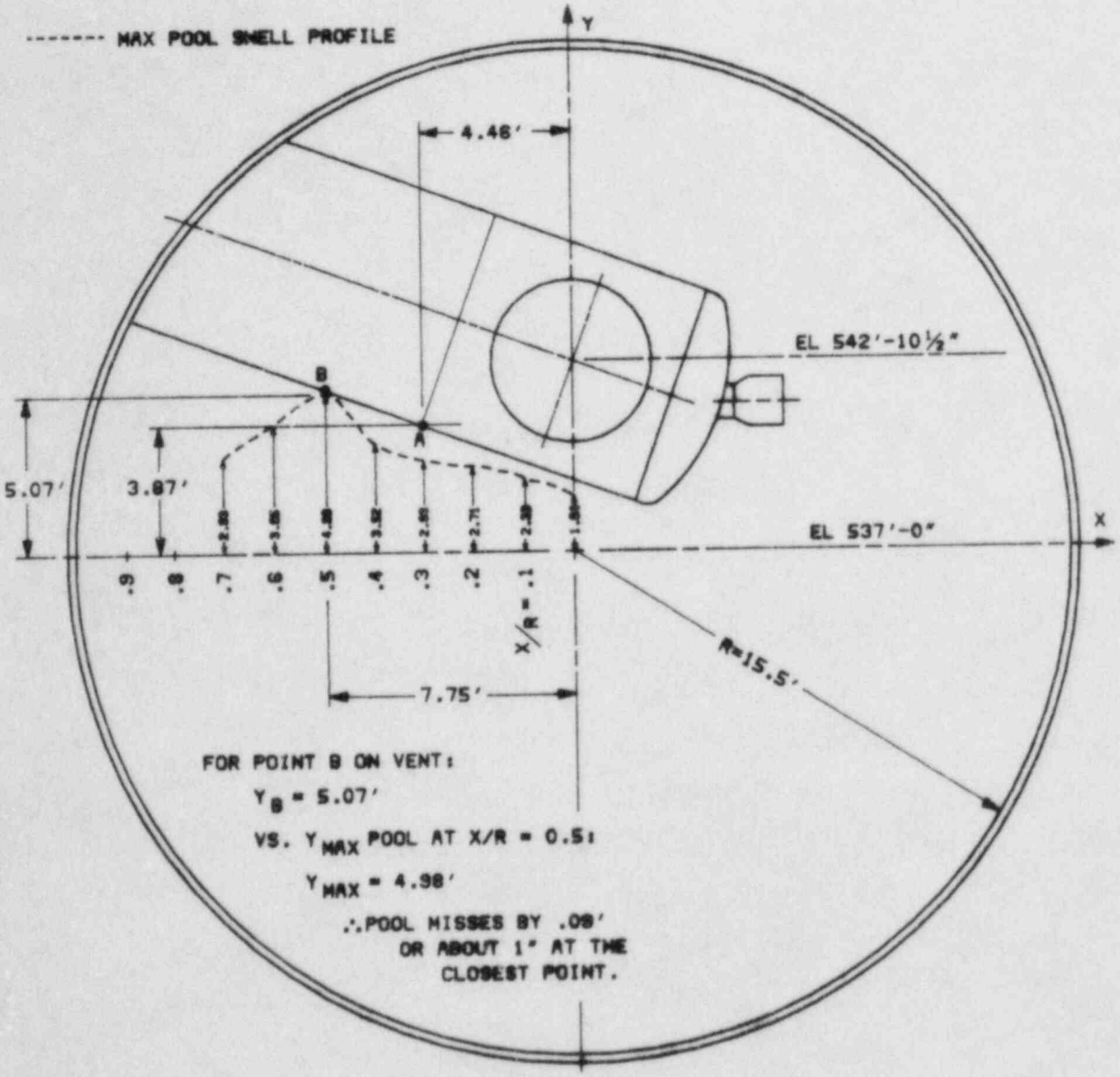

FIGURE BNL-22-1
TYPICAL MID VENT BAY CROSS-SECTION

BFN PUAR

APPENDIX I

FINAL TVA RESPONSES TO NRC AND FRANKLIN RESEARCH CENTER QUESTIONS

General Response to PUAR Questions

BFN LTP analysis and design activity has proceeded on a schedule necessary to support installation of all modifications during the Cycle 4 and 5 refueling outages of each unit, as required by NRC. The first BFN Cycle 4 refueling outage began in April 1981, and most of the major modification designs were complete by May 1981. Remaining modification designs, primarily for torus attached piping external supports, were complete in time to support installation during the Cycle 5 refueling outages.

In order to satisfy schedule commitments, it was necessary to make interpretations of LDR and NUREG 0661 requirements based upon the best available information at the time of analysis. Most of the interpretations were originally established in 1979 and early 1980. A continuing effort to remove excessive conservatism from load definitions and analysis methods was made, particularly when that conservatism would result in unnecessary, impractical modifications.

When later information on load definitions and associated analysis methods became available, it was compared to the previous interpretations. The later information was used for reanalysis and associated design work if a significant unconservatism in the previous interpretation was indicated. For example, the final downcomer tiebar/v-bracing modification resulted from November 1981 changes in the DBA condensation oscillation lateral load definition.

Sometimes, later information was used to remove excessive conservatism in remaining analysis and design work. For example, the 1.1 SRSS load combination technique was permitted for torus attached piping analysis after NRC's final position on this subject was defined in April 1983 by PUAR Reference 58. An absolute summation combination technique was required prior to that time.

Finally, when the later information showed the previous load definitions and analysis methods to be adequately (but not excessively) conservative, the original interpretations were retained. In these situations, reanalysis utilizing the later information would have been unnecessary and costly, and, in some cases, would have resulted in delays in the installation of modifications.

Many of the PUAR questions derive from situations where the original interpretations stated in PUAR Section 4 were used for analysis. Justification for these interpretations was provided in PUAR Section 4, Section 5, and Appendix C. Additional technical justification follows in the responses to specific questions on these topics. Other PUAR questions simply request additional information, which is provided in the responses.

It is TVA's position that the BFN PUAR and our review question responses demonstrate compliance with the intent of the Mark I Containment Long-Term Program and NUREG 0661 (i.e., to upgrade the containment system safety margins, for all postulated hydrodynamic loading conditions, to those intended by the original design specifications). On this basis, we feel that all indicated safety concerns are fully and satisfactorily addressed, and we respectfully request a favorable final evaluation for the BFN LTP.

ITEM 1:

Provide a more detailed description of the vent system analysis regarding downcomer lateral loads (Section 4.4.5 (5)).

RESPONSE:

As described in the LDR, the condensation oscillation lateral load is simulated for each downcomer pair by adding a differential pressure for one downcomer to the internal pressure, that occurs in both downcomers, thereby producing a higher load in one downcomer than in the other. Thus, from Figure 4.4.3.4 of the LDR, a darkened downcomer indicates that the differential and internal pressures are working simultaneously, whereas the other downcomer only experiences the internal pressure.

A 45° beam model, Figure 6-2, was used to analyze both IBA CO and DBA CO. Based on the primary downcomer swing frequency extracted from a modal analysis of the system, sinusoidal forcing functions were applied to the downcomer pairs considering the load cases defined by Figure 4.4.3-3 in the LDR. Since the primary swing mode for the BFN System occurs in the 8 Hz range, the 1st, 2nd, and 3rd harmonics were addressed by sinusoidal functions in the 4, 8, and 12 Hz ranges, respectively. An added conservatism in the BFN analysis was the application of the first harmonic forces to the coincident 8 Hz swing frequency. The response of the system to this single frequency load enveloped responses from the sum of the three harmonics defined by the LDR. Also, the first harmonic force amplitudes were applied with 16 and 24 Hz sinusoidal functions to verify that higher frequency responses do not impact the total CO response. In fact, 30 individual sinusoidal functions were applied for each load case to account for potential harmonics at the 1/2, 1, 1-1/2, 2, and 2-1/2 harmonics of the six discreet primary swing mode frequencies in the 8 to 9 Hz range.

The BFN vent system was analyzed for the four initial differential pressure cases specified by a May 1981 draft of LDR Section 4.4.3. (See PUAR Figure 6-12.) Subsequently, four additional mirror image cases were included in the final CO lateral load definition. Evaluation of both the initial four cases and their four mirror images demonstrated

that Load Case 1 is controlling and additional rigorous analysis of the mirror images was unnecessary. (See response to BNL Item 11 for further discussion.) The DBA CO downcomer lateral load effects were combined with DBA CO fluid drag loads and other loads in the controlling load combinations and evaluated to the governing stress levels.

The chugging lateral loads were calculated in accordance with the LDR and NUREG 0661, using frequencies from the modal analyses performed on the 45° and 180° vent system beam models. These loads were applied to single downcomers chugging exclusively and to multiple downcomers chugging synchronously. The 45° beam model (PUAR Figure 6-2) was used for analysis of single downcomer chugging lateral loads, and the 180° beam model (PUAR Figure 6-3) was used for analysis of downcomer synchronous chugging lateral loads. The resulting effects were then combined with other loads, including chugging fluid drag loads on the tiebars and V-bracing for stress and fatigue evaluation of the entire vent system.

Stresses were determined by applying appropriate intensification factors at intersections and by direct application of loads to finite element models shown on PUAR Figures 6-5, 6-7, and 6-11.

ITEM 2:

Provide the physical details of the seismic lugs that restrain the torus against horizontal seismic motion yet allow thermal growth.

RESPONSE:

The erection drawing for the seismic lugs is PDM-E12. Fabrication details for the components are shown on PDM drawing 41. (Copies of the drawings are available for review.)

ITEM 3:

Indicate how the ring girders were analyzed for loads from attached internal structures. Any dynamic load factors that may have been used in the analysis must be provided and justified.

RESPONSE:

The effects of the larger systems on the ring girder and other portions of the torus were considered as follows:

1. Vent System: The support column reactions due to vent header pool swell impact were considered directly, as described in Section 5.4.2.7 of the PUAR. In addition, the vent system masses were included in the dynamic 22-1/2° torus model, so that the mass times acceleration (rigid body) inertial effects were developed for all dynamic loads.

2. ECCS Header: The torus cradle stresses due to the reaction loads at the ECCS header supports were added to the stress intensities in that region for the torus model, without exceeding allowables. The mass of the ECCS was also included in the dynamic torus model. Thus, the rigid body portion of the ECCS header support reactions were conservatively included twice.

3. HPCI and RHR: The masses of these systems were also included in the dynamic torus model.

The other systems were judged not to affect overall torus behavior, but to produce only localized effects. Support connections to the ring girder were heavily reinforced. The line-of-action of pipe bracing members was applied near the base of the ring girder to eliminate any significant overturning tendency. For example, see PUAR Appendix G Plates 18 and 21. Additionally, the support system for S/RV discharge lines and quenchers includes a 15-inch x 15-inch box-beam which forms a continuous ring inside the torus and prevents any possibility of overturning each ring girder in the region of attachment. The main support members for the catwalk perform a similar function at each ring girder. See PUAR Plates 12, 13, 26, and 27.

Local acceleration response spectra for each dynamic load were defined at each ring girder attachment point. The attached piping systems and structures were analyzed for these input spectra and associated displacements.

Reactions were calculated from the piping analyses per Sections 7 and 8 of the PUAR, and for the catwalk per Section 9. The local reinforcement was designed for these reactions. The localized stresses transmitted to the ring girder were limited to 3 ksi. When combined with the general ring girder stresses, no allowables were exceeded.

ITEM 4:

With respect to the 22-1/2° torus model mentioned in Section 5.4.1.1 of the PUAR (5), the boundary conditions are based on the assumption that all loads are applied equally to each of the 16 segments. However, the safety-relief valve and chugging loads are asymmetrical. Justify the use of a 22-1/2° model to evaluate the torus for S/RV and chugging instead of the 180° model required by the criteria (1).

RESPONSE:

The following points pertain:

1. Symmetric loading, for S/RV and chugging, is certainly bounding for cradle loads just from the point of view of the magnitude of the net applied load.

2. Shell responses are primarily a localized phenomenon. They can be affected by ring girder ovalling, but this too is related to the net load, and so would be more severe for symmetric loads.

3. The BFN torus support system inhibits asymmetric response. The development of asymmetric modes would require longitudinal motion of the torus, which is prevented by the seismic lugs. It would also require radial movement of the ring girders which is prevented by the torus snubbers (PUAR Plate 1). Friction at the cradle support pads would also inhibit any tendency for asymmetric response.

4. If significant asymmetric response could develop, it would have been present in the single- and multi-valve S/RV tests. None was evident, and analysis results based on symmetric loading boundary conditions were shown to be conservative (PUAR Appendix C).

Finally, it is important to recognize that Section 6 of the PUAAG (Reference (1) of the questions) is not a criteria. It is a guideline for analysis methods.

ITEM 5:

Figure 5-6 in the PUAR (5), which depicts the 180° model of the torus, shows only the lower half of the torus shell. Indicate whether the model includes the torus supports.

RESPONSE:

Figure 5-6 of the PUAR depicts only the lower half of the 180° model for clarity. The actual model includes the upper and lower halves. All supports are included (i.e., the torus snubbers, seismic lugs, and the support pad-tiedown system).

ITEM 6:

Since NRC Regulatory Guide 1.61 (4) deals with damping values for the seismic design of structures, explain how this Regulatory Guide validates the use of 4 percent damping for the 0.0 ΔP pool swell analysis of the torus (Section 5.4.2.7 (5)).

RESPONSE:

The use of NRC Regulatory Guide 1.61 damping was accepted for analysis by Section 4.4.2 of NUREG 0661, and the 0.0 ΔP pool swell case was designated as a Service Level D condition by Section 4.3.3.1 of NUREG 0661. Regulatory Guide 1.61 specifies 4 percent damping for welded steel structures under SSE loading which is normally associated with Service Levels C and D conditions. The torus and vent system are welded steel structures.

Two percent damping was conservatively used for BFN vent system 0.0 ΔP pool swell analysis. Four percent damping was used for the torus. This assumption in combination with the overall analysis method produced a reasonably conservative dynamic response prediction. BNL Items 1 through 4 provide additional information on the BFN pool swell analysis method.

Finally, it is noteworthy that two percent damping was conservatively assumed for all Service Level C load combination torus and vent system analyses, to reduce the number of cases for analysis. Four percent damping is considered justifiable for the Service Level C and D load combinations on the basis of Regulatory Guide 1.61.

ITEM 7:

With respect to Section 5.4.2.11 of the PUAR (5), provide the technical basis and justification for considering the forcing functions from 0 to 30 Hz instead of the full 0 to 50 Hz for post-chug analysis of the torus.

RESPONSE:

The intent of the discussion in Section 5.4.2.11 of the PUAR was to emphasize the following major points:

1. There are significant conservatisms in the BFN post-chug analysis method which offset the effects of not considering the harmonics in the 30 to 50 Hz range.

2. The 30 to 50 Hz harmonics were considered in the drag load analyses. (See Section D.1.2.4.1 of the PUAR.)

3. Pre-chug generally controls over post-chug for torus analysis. The BFN pre-chug analysis was performed in complete accordance with NUREG 0661 and the LDR, including additional conservatisms inherent in the method.

4. Any remaining concern with the response of high frequency modes for torus attachments is offset by the high frequency content in the pool swell analyses.

Finally, a strong empirical indication (not a rigorous analytical proof) of the conservatism of the BFN chugging analyses (both pre- and post-chug) is seen in the attached table. BFN shell surface stress and support reaction forces are presented, factored as nearly as possible to an FSTF-equivalent basis, and compared to measured and calculated NEP values for the FSTF. The conservatism of the BFN responses to post-chug analysis results is primarily due to the absolute summation of all 30 harmonics in the 0 to 30 Hz range. (Note that the dominant BFN torus modes are in the 0 to 30 Hz range.) PUAR Reference 20 recommends absolute summation of 5 harmonics plus SRSS of remaining harmonics to achieve an 84 percent NEP.

TABLE FRC-7-1

COMPARISON OF FSTF AND BROWNS FERRY CHUGGING RESPONSES

RESPONSE	BFN CALCULATED RESULTS		BFN RESPONSES FACTORED TO EQUIVALENT FSTF		MAXIMUM FILTERED FSTF, PRE- AND POST-CHUG, PER REF.20 TABLE 5-1	DUE TO POST-CHUG ONLY	
	PRE-	POST-	PRE-	POST-		50% NEP FSTF, PER REF.20 TABLE 4-1	84% NEP FSTF, PER REF.20 TABLE 4-1
BOC SURFACE STRESS INTENSITY (KSI)	1.10	1.12	1.31	1.33	0.90	0.88	0.98
INSIDE REACTION (KIPS)	102	100	57	56	31.2	17.0	19.2
OUTSIDE REACTION (KIPS)	113	110	64	62	32.3	17.7	20.2

(1) FSTF EQUIVALENT SHELL STRESS INTENSITY = $S_{BFN}\left[\frac{(R/T)FSTF}{(R/T)BFN}\right] = 1.19\ S_{BFN}$

WHERE, R = MINOR RADIUS OF THE TORUS, T = SHELL THICKNESS, AND S = STRESS INTENSITY

(2) FSTF EQUIV. SUPPORT REACTIONS = (BFN REACTION) $\left(\frac{\text{FSTF POOL AREA PER COLUMN PAIR}}{\text{BFN POOL AREA PER CRADLE}}\right)$

= 0.562 (BFN REACTION)

ITEM 8:

Items 2 and 3 in Section 5.4.2.11 of the PUAR (5) suggest that the pre-chug load bounds the post-chug load in the analysis of the torus; however, Item 5 in Section 5.4.2.11 indicates a higher surface stress for post-chug. Explain this apparent inconsistency and indicate whether pre-chug or post-chug was considered in the controlling load combinations for the torus.

RESPONSE:

The discussion of Item 5 in Section 5.4.2.11 of the PUAR demonstrates the inherent conservatism of the BFN post-chug analysis, relative to the FSTF data. The discussion of Items 2 and 3 of 5.4.2.11 show that the LDR prescribed pre-chug analysis method bounds the actual measured FSTF chugging responses due to both the pre- and post-chug phases. This is not to say that pre-chug will always bound post-chug. It only says that consideration of the pre-chug phase alone is sufficient to demonstrate the conservatism of torus results based on the LDR method as compared to actual measured FSTF results for the combined pre- and post-chug phases. Also see the response to FRC Item 7, including Table FRC-7-1.

For all load combinations involving chugging, the maximum stress due to either pre-or post-chug was used (i.e., an envelope of pre- and post-chug responses).

ITEM 9:

With respect to the fatigue analysis of the torus presented in Section 5.4.6 of the PUAR (5), specify the elasticity methods used to calculate stress intensification factors at the penetrations.

RESPONSE:

The stress intensification factors presented in Section 5.4.6 of the PUAR were calculated using formulas presented in the following text: Formulas for Stress and Strain, 5th edition, by R. J. Roark and W. C. Young, McGraw-Hill. The insert pad to shell junction intensification factor was based on Case 14, page 598. For the insert pad to nozzle junction, Case 5, page 593 was used.

ITEM 10:

Provide and justify the bounding technique used to determine the controlling load cases presented in the PUAR (5) in the following sections:

5.5.1, page 5-21
6.3.2 (and Table 6-5), page 6-6
6.4.2 (and Table 6-7), page 6-7
6.5.2 (and Table 6-9), page 6-8
6.7.2 (and Table 6-12), page 6-12
6.8.2 (and Tables 6-15 and 6-16), page 6-14
6.9.2 (and Tables 6-17, 6-18, and 6-19), page 6-15
7.3.1 (and Table 7-1), page 7-7
7.4.1 (and Tables 7-2 to 7-4), page 7-12
8.2.22 (and Table 8-2), page 8-3
9.1, page 9-2
9.2, page 9-2

RESPONSE:

PUAR Section 5.5.1

No bounding techniques were used for determining controlling load cases for the torus analysis. All load combinations were analyzed, including the calculation of stress intensities and reaction loads for the cradle and torus snubbers. The referenced section was stating which of the combinations produced the highest stress intensities.

PUAR Sections 6.3.2 through 6.9.2

PUAR Tables 6-5, 6-7, 6-9, 6-12, 6-15, 6-17, 6-18, and 6-19 give the event, combination, and service level of the various locations of inspection. Table 3-1 of the PUAR shows this information in a different form. The bounding technique for the tables in PUAR Section 6 was such that Service Level C event combinations would be qualified using Service Level B allowables when possible. When this was not possible, actual service level combinations coincided with the assigned service level stress limits in PUAR Table 3-1.

A logic description of the bounding justification for each table follows:

PUAR Table 6-5 Logic

- Load Combination (LC) 15 to Service Level (SL) B allowables envelops LC 1 through LC 14.
- LC 27 to SL B allowables envelops LC 17, LC 20, LC 21, LC 23, and LC26.
- LC 25 to SL B allowables envelops LC 16, LC 18, LC 19, LC 22, and LC24.
- IBA is not indicated in LC 15 because:

  (1) SBA chugging is no less severe than IBA chugging.

  (2) IBA CO is enveloped by DBA CO in LC 27.

PUAR Table 6-7 Logic

- LC 18 to SL B allowables envelops LC 16.
- For the vacuum breaker to main vent cap intersection, dynamic loading due to pool swell vent response far exceeds any chugging, CO, or S/RV effect. Therefore, evaluation of LC 1 through LC 15 plus LC 17, LCs 20 through 23, and LCs 26 through 27 is not necessary.
- LC 18 does not envelop LC 19, LC 24, and LC 25. However, the load contribution from SSE versus OBE and the S/RV contribution are small and have been neglected considering the increased allowable for SL C relative to SL B.
- Note that the pool swell load considers pool swell vent response and direct impact of the swell on the vacuum breaker shell. (The vacuum breaker shell is actually partially shielded by the vacuum breaker access platform.)

PUAR Table 6-9 Logic

- This logic is similar to PUAR Table 6-5 except LC 27 could not be satisfied for SL B primary plus secondary stresses ($P_L + Q < 3\ S_{mc}$). Therefore, LC 21 was evaluated for primary plus secondary instead. (LC 21 is the same as LC 27 with no S/RV. PUAR Table 6-9 incorrectly indicated LC 27 instead of LC 21. This correction was made in PUAR revision 2.)

PUAR Table 6-12 Logic

- Again this logic is similar to PUAR Table 6-5 except LC 27 would not meet SL B allowables. Therefore, LC 27 was evaluated to SL C allowables and LC 21 was evaluated to SL B allowables for both primary and primary plus secondary stresses. (PUAR Table 6-12 incorrectly indicated LC 27 instead of LC 21 for the Service Level B combinations. This correction was made in PUAR revision 2.)

PUAR Tables 6-15 and 6-16 Logic

- Again this logic is similar to PUAR Table 6-5. The noted loads are the worst possible combination of any accident condition, including thermal effects, and the buckling evaluation is performed on this basis.

PUAR Tables 6-17, 6-18, and 6-19 Logic

- Again, LC 15, LC 25, and LC 27 are the worst case load combinations for the system. The indicated stresses are maximum surface including secondary effects with significant margin against 1.5 S_{mc}. Therefore, the primary plus secondary stress range evaluation is automatically assured.

PUAR Section 7.3.1

Section 7.3.1 provides a general description of the bounding technique that was used to determine controlling load cases for S/RV piping in the drywell at Browns Ferry. Specifically, the controlling load cases for drywell S/RV piping were determined by the following process:

(1) Survey all defined normal, seismic, and LOCA load definitions to determine which of these have significant effect on drywell S/RV piping.

Note that separate models of the piping systems were developed to analyze the drywell and wetwell portions of the system. The wetwell models were developed in significant detail to study torus hydrodynamic phenomenon closely. These models extended a significant distance into main vent to account for attenuation. It was found that the S/RV piping in the main vent is isolated from most of the hydrodynamic effects of S/RV discharge or LOCA excitation of the suppression pool. (An exception to this is the containment vent response

induced by DBA LOCA pool swell.) The drywell piping is sufficiently removed from the suppression pool to discount effects from water clearing transients in wetwell portions of the S/RV lines.

The load sources that were determined to have a significant effect on drywell S/RV piping are:

a. Deadweight

b. Seismic - OBE and SSE

c. All S/RV blowdowns

d. Pool swell vent response

e. Thermal expansion

f. Pressure

(2) Perform an inspection of Table 5-2 in the PUAAG (PUAR Reference 13) considering the resultant S/RV load sources noted in step 1 above.

A summary of the findings with respect to PUAR Table 7-1 follows.

Case 1: Satisfies LC 1.

Case 2: Satisfies LC 3 which envelops LC 2.

Case 3: Satisfies LC 15 which envelops LC 4 through LC 14 except as indicated by note 6 on PUAR Table 7-1.

Case 4: Satisfies LC 27 which envelops LC 16 through LC 26.

PUAR Section 7.4.1

Section 7.4.1 provides a general discussion of the bounding technique for wetwell S/RV piping. All load sources are treated. A summary of the enveloping logic for PUAR Tables 7-2, 7-3, and 7-4 with respect to Table 5-2 of the PUAAG (PUAR Reference 13) is listed below.

PUAR Table 7-2

Case 1 and Case 2: Satisfies LC 1.

Case 3 and Case 4: Satisfies LC 3 which envelops LC 2.

PUAR Table 7-3

Case 1 and Case 2: Satisfies LC 11, row 11, which envelops LC 4 through LC 10 for row 11.

Case 3 and Case 4: Satisfies LC 15, row 11, which envelops LC 12 through LC 14 for row 11.

Case 5 and Case 6: Satisfies LC 15, row 10, which envelops LC 4 through LC 14 for row 10.

PUAR Table 7-4

Case 1: Satisfies LC 27 which envelops LC 17, LC 20, LC 21, LC 23, and LC 26. (Note that CO and chugging do not occur simultaneously and chugging is addressed more conservatively in PUAR Table 7-3 for SBA/IBA events.)

Case 2: Satisfies LC 25 which envelops LC 16, LC 18, LC 19, LC 22, and LC 24.

Case 3: Satisfies LC 16 for the 0.0 ΔP case. (Due to the low probability of occurrence, S/RV blowdown and earthquake are not assumed to be concurrent with the 0.0 ΔP pool swell. This is in accordance with the PUAAG.)

PUAR Section 8.2.2.2

The boundary technique used to reduce the number of load case combinations shown in PUAAG Table 5-2 (PUAR Reference 13) to those shown in PUAR Table 8-2 was based on using the most conservative combination of load cases associated with each of the service levels and ASME Section III, NC-3600 (PUAR Reference 68) equation 9 stress limits. (Note that for different local combinations, the stress limits could be 1.2 S, 1.8 S, or 2.4 S, corresponding to Service Levels B, C, and D, respectively.) The following are two examples of how this bounding technique was applied:

(1) When two series of load combinations listed in the PUAAG were the same except that one included OBE and the other SSE and both sets of load combinations had the same stress limits, the OBE and SSE load cases were enveloped. In this way the two sets of load combinations could thus be reduced to one.

(2) Another example would be when one set of load combinations consisted of all the load cases found in another set of load combinations plus at least one more load case. If both sets of load combinations had to meet the same stress limits then only the combination with the greater number of load cases was evaluated.

The controlling load combinations for each service level equation 9 stress limit were found in this way. In addition, NC-3600 equation 10 or 11 was satisfied for each of the controlling load combinations.

PUAR Section 9.1

The new catwalk finite element model was analyzed for all applicable load events. The results showed that the largest stresses, by far, were due to pool swell impact and drag. Therefore, the most severe condition involving this load was limiting. For Load Combination 25, the effects of pool swell impact-drag, pool swell and vent header motions, S/RV motions, deadweight, and SSE were added absolutely.

PUAR Section 9.2

In the same manner as the catwalk, the vacuum breaker valve platform is most severely affected by pool swell impact-drag loads, and the limiting load combination was determined in the same way.

ITEM 11:

Provide the stress results from the analysis of the torus shell and supports.

RESPONSE:

Stress intensities were calculated by postprocessor computer codes for all load combinations and for all elements in the finite element model. The results were screened to locate predicted overstresses. Following modifications, all stresses were below allowables.

The most highly stressed torus support locations are in the cradle, adjacent to the scab plates described in Section 5.2.4.3 of the PUAR. The addition of the scab plates reduced the local cradle stresses for Load Combination 14 from 24.4 ksi to 19.7 ksi. Relative to the Service Level B allowable of 21.6 ksi (see Section 5.3.2 of the PUAR), the stress factor was reduced from 1.13 to 0.91. The maximum stress for any Service Level C or D load case was in the same region of the cradle and was due to Load Combination 25. Even without the scab plates, however, the maximum stress intensity was 26.8 ksi, compared to the 28.8 ksi allowable. These cradle stress results conservatively neglect the S/RV load reduction factor for torus supports defined in PUAR Section C.9.1.

The shell and ring girder stress allowables presented in Table 5-1 of the PUAR were never approached except in the vicinity of large piping penetrations. A number of the piping modifications described in Section 8, as well as the nozzle reinforcements and local shell reinforcement around the ECCS header penetrations were required in order to meet the containment vessel (ASME Section III, Subsection MC) allowables. At some of these locations, the calculated stresses are greater than 90 percent of Service Level B allowables for the primary plus secondary stress intensity range.

An indication of the general shell stress state away from the influence of penetration loads is given by the following table. Membrane and surface stress intensities are presented for mid-bay bottom-dead-center, one of the more highly stressed locations, for the most critical load combinations.

Load Comb.	Service Level	Stress Intensity (ksi)		% of Allowable	
		Membrane	Membrane + Bending	Membrane	Membrane + Bending
14	B	15.1	15.4	78	53
18	B	5.1	5.4	26	19
20	B	9.4	9.9	49	34
25	C	8.9	9.3	23	16
27	C	13.3	13.9	35	24
16B	D	6.2	6.8	15	11

ITEM 12:

Regarding the analysis of the main vent/drywell intersection, clarify whether the seismic and thermal response of the drywell was considered (Sections 6.2.1.2.7 and 6.2.1.2.9 (5)).

RESPONSE:

Thermal growth of the containment shell was considered in the analysis of the main vent/drywell intersection. Thermal displacements were calculated for the drywell based upon maximum air temperatures occurring during the DBA, IBA, and SBA events. These displacements were input at the nodes representing the drywell/main vent intersection. The thermal analysis was then completed considering expansion and restraint of free end displacement of the vent system.

The BFN LTP seismic analysis was based upon the methods employed in the original plant design. Seismic response of the drywell/main vent intersection was analyzed using equivalent static loads determined from appropriate acceleration levels of the vent system. This is consistent with the general guidelines of NUREG 0661, Section 4.4.1 as well as the PUAAG (PUAR Reference 13).

ITEM 13:

Provide a summary of the analysis of the vacuum breaker valves; indicate whether they are considered Class 2 components as required by the criteria (1).

RESPONSE:

Apparently this request relates to analysis of the drywell/wetwell vacuum breakers for cyclic loads occuring during chugging events. Since this concern is not part of the Mark I Containment Long-Term program, a separate response was sent to the NRC on November 5, 1984 (NEB 841113615).

If this request relates to the new 10-inch S/RV vacuum breakers, these valves have been analyzed and subsequently modified to satisfy ASME Section III Class 2 stress limits for all postulated conditions including opening impacts. The modified S/RV vacuum breakers are shown on TVA drawing 47W401-9.

ADDENDUM

Additional information on qualification testing of the modified S/RV vacuum breakers for opening impact loads was requested during the September 13, 1984 meeting with NRC and FRC representatives. That information follows:

Preliminary forcing functions for design of opening impact modifications were based on conservative predictions extrapolated from Monticello test results. Modification designs were made and preliminary tests for short-term adequacy were conducted on that basis.

The final forcing function for the S/RV line E vacuum breaker was determined from discharge line pressure measurements taken during the April 1983 BFN S/RV tests (PUAR Reference 41). This forcing function was analytically extrapolated for all BFN S/RV lines and all long-term program load conditions. Then a prototype vacuum breaker was tested at Wyle Laboratory, Huntsville, Alabama, to demonstrate operability for all forcing functions and the full 40-year plant life.

ITEM 14:

The PUAR (5) indicates that the calculated stress values at the following locations are very close to the respective allowables:

- o downcomer/vent header intersection (Section 6.5.4.1)
- o downcomer/tiebar intersection (Section 6.7.4.1)

Indicate conservatisms in the analysis to show that these calculated values would not be exceeded if a different analytical approach were to be used.

RESPONSE:

Although the stress values at the intersections mentioned above were close to the respective allowable stresses, this should not represent a significant concern. Design modifications were made such that the stresses resulting from the new configurations were just below the acceptable values. This would normally be anticipated.

There are conservatisms which could be removed to obtain a greater difference in the allowable and actual calculated stress values for the above intersections. For example:

(1) Absolute summation was used in the combination of loads.

(2) The downcomer/tiebar was conservatively analyzed using Service Level B allowables for Service Level C loads. (SSE seismic loads were included in the actual loading in place of the prescribed OBE seismic load.)

(3) There are other conservatisms associated with the DBA CO lateral load analysis method as described in the response to FRC Item 1.

ITEM 15:

Stress intensification factors for the miter bends in the vent system are not found in Table 6-17 as stated in Section 6.9.1 of the PUAR (5). Provide these factors.

RESPONSE:

Main vent miter bend SIF - 3.85

Vent header miter bend SIF - 8.2

Downcomer miter bend SIF - 3.82

(See Table 6-21 of revision 2 of the PUAR.)

ITEM 16:

Regarding the torus bellows analysis in Section 6.10.1.1 of the PUAR (5), provide the method and technical basis for calculating the spring values that represent the bellows flexibility in the computer models of the vent system (Figures 6-2 and 6-3 (5)).

RESPONSE:

The spring values that represent the bellows flexibility were calculated using the "Standards of the Expansion Joint Manufacturers Association, Inc." (PUAR Reference 24). Appropriate data for the BFN bellows was input including convolution depth, thickness, number of convolutions, and modulus of elasticity.

ITEM 17:

Provide and justify the approach for the fatigue evaluation of the bellows mentioned in Section 6.10.3 of the PUAR (5).

RESPONSE:

The fatigue evaluation was carried out using "Standards of the Expansion Joint Manufacturers Association, Inc." (PUAR Reference 24) and the Mark I Containment Program Augmented Class 2/3 Fatigue Evaluation Method and Results for Typical Torus Attached and S/RV Piping Systems (PUAR Reference 21). Deflections for the torus and bellows were obtained for each load event using computer analysis results and hand calculations. These deflections resulted in bellows stresses which were then combined in accordance with the fatigue evaluation method noted above.

ITEM 18:

According to Section 7.3.3.1 of the PUAR (5), the safety-relief valve line penetration of the main vent was modeled using cylindrical shell flexibility characteristics. Indicate the method for determining these characteristics.

RESPONSE:

For the S/RV line penetration of the main vent, a six degree of freedom "support" was modeled. For three degrees of freedom (pipe torsion and the two translational shear directions) full fixity was assumed. For the circumferential and longitudinal bending directions, Bijlaard's methods (PUAR Reference 64) were utilized to determine rotational spring rates. For the main vent radial direction, a translational spring rate was determined per the R. J. Roark text, Formulas for Stress and Strain.

ITEM 19:

Provide the technical basis for obtaining the stress intensification factors used in the analysis of the safety-relief valve discharge piping system (Sections 7.3.3.1 and 7.4.3.1 (5)).

RESPONSE:

In general, the 1977 ASME Code Section III (Figure ND-3673.2(b)-1) is the technical basis for the stress intensification factors utilized in the S/RV discharge piping analysis with the following exceptions:

Component	Basis
Weld-O-Let	Bonny Forge stress intensification factors and stress indices for weld-o-lets.
Sweep-O-Let	Stress intensification factors and stress indices for the Bonny Forge sweep-o-lets.
Quencher Near Collar Support	Stress intensification factor based on effective section of quencher. Assumes hole zone of quencher provides no structural contribution. $i = \frac{\text{Section modulus of 12 inch Sch 80 Pipe}}{\text{Effective section modulus of quencher}}$

ITEM 20:

Provide the stress results from the wetwell and drywell safety-relief valve discharge piping analysis (Sections 7.3.4.1 and 7.4.4.1 (5)).

RESPONSE:

Tables FRC-20-1 through FRC-20-4 provide a summary of the maximum equation 9 stresses from the S/RV discharge piping analysis.

TABLE FRC-20-1

DRYWELL LOAD COMBINATIONS - MAXIMUM STRESS

	LOAD CASE (1)	NODE	STRESS (KSI)	STRESS RATIO (3)
LINE C (2)	CASE 1	59	17.8	0.991
	CASE 2	59	20.5	0.760
	CASE 3	47	22.1	0.613
	CASE 4	59	20.6	0.573
LINE E (2)	CASE 1	157	16.2	0.898
	CASE 2	157	23.8	0.883
	CASE 3	157	23.8	0.662
	CASE 4	157	23.9	0.664

1. LOAD CASE PER TABLE 7-1 OF PUAR.

2. LINE C IS A REPRESENTATIVE SHORT LINE.
   LINE E IS A REPRESENTATIVE LONG LINE.

3. STRESS RATIO = $\frac{\text{CALCULATED STRESS}}{\text{ALLOWABLE STRESS}}$

TABLE FRC-20-2

NOC - SERVICE LEVEL B AND C LOAD COMBINATIONS
MAXIMUM STRESSES - WETWELL EVALUATION

	LOAD CASE (1)	NODE	STRESS (KSI)	STRESS RATIO (4)
LINE L (3)	CASE 1	ENVELOPED BY CASE 2 (2)		
	CASE 2	2	10.3	0.573
	CASE 3	ENVELOPED BY CASE 4 (2)		
	CASE 4	2	10.9	0.404
LINE H (3)	CASE 1	ENVELOPED BY CASE 2 (2)		
	CASE 2	8	13.3	0.758
	CASE 3	ENVELOPED BY CASE 4 (3)		
	CASE 4	8	14.1	0.522

1. LOAD CASES PER TABLE 7-2 OF PUAR.
2. THE ENVELOPING OCCURS BECAUSE A WORST CASE NOC - BLOWDOWN (SCREENED BETWEEN FIRST AND SECOND ACTUATION) IS USED FOR THE STRESS ANALYSIS.
3. LINE L - TYPICAL SHORT LINE.
   LINE H - TYPICAL LONG LINE.
4. STRESS RATIO = $\frac{\text{CALCULATED STRESS}}{\text{ALLOWABLE STRESS}}$

TABLE FRC-20-3

SBA/IBA - SERVICE LEVELS C AND D LOAD COMBINATIONS
MAXIMUM STRESSES - WETWELL EVALUATION

	LOAD CASE [1]	NODE	STRESS (KSI)	STRESS RATIO [3]
LINE L	CASE 1	12	21.6	0.887
	CASE 2	2	24.9	0.922
	CASE 3	ENVELOPED BY CASE 5 [2]		
	CASE 4	ENVELOPED BY CASE 6		
	CASE 5	12	21.8	0.674
	CASE 6	2	26.8	0.745
LINE H	CASE 1	8	26.5	0.982
	CASE 2	8	26.0	0.963
	CASE 3	ENVELOPED BY CASE 5		
	CASE 4	ENVELOPED BY CASE 6		
	CASE 5	10	31.7	0.881
	CASE 6	8	32.2	0.994

1. LOAD CASES PER TABLE 7-3 OF PUAR.
2. SBA AND IRA BLOWDOWNS SCREENED TO PROVIDE WORST CASE FOR ANALYSIS.
3. STRESS RATIO = $\frac{\text{CALCULATED STRESS}}{\text{ALLOWABLE STRESS}}$

TABLE FRC-20-4

DBA - SERVICE LEVEL D LOAD COMBINATIONS
MAXIMUM STRESSES - WETWELL EVALUATION

	LOAD CASE (1)	NODE	STRESS (KSI)	STRESS RATIO (2)
LINE L	CASE 1	235	22.4	0.692
	CASE 2	1	33.4	0.927
	CASE 3	1	31.7	0.880
LINE H	CASE 1	8	28.1	0.781
	CASE 2	8	28.3	0.787
	CASE 3	48	27.4	0.760

1. LOAD CASES PER TABLE 7-4 OF PUAR.

2. STRESS RATIO = $\frac{\text{CALCULATED STRESS}}{\text{ALLOWABLE STRESS}}$

ITEM 21:

Provide and justify the allowable safety-relief valve nozzle loads which were referred to in Section 7.3.4.2 of the PUAR (5).

RESPONSE:

As summarized in the PUAR, relief valve nozzle loads calculated in the drywell S/RV piping analysis were compared to a set of allowable nozzle loads used in the original S/RV analysis performed by Teledyne Engineering Services and documented by PUAR Reference 45. These allowable loads were provided by the relief valve vendor, Target Rock, and are incorporated in the design report for this component. The allowables and worst case calculated loads are:

Valve Flange	Worst Load*	Allowable Resultant Bending Moment from Dynamic Loads
Inlet	320,961 IN-LB	400,000 IN-LB
Outlet	287,568 IN-LB	300,000 IN-LB

*SRSS combination of dynamic loads.

In addition to the vendor allowable nozzle load check, the connecting flanges for the relief valve installation were evaluated against static and static plus dynamic load allowables as calculated per the procedure of Paragraph NB-3658.1 in the 1977 ASME Boiler and Pressure Vessel Code (PUAR Reference 68). The following table provides a summary of that evaluation:

Valve Flange	Condition	Worst Load (IN-LB)	Allowable (IN-LB)
Inlet	S	296843	437321
Outlet	S	306205	372971
Inlet	S + D (B)	390466	874642
Outlet	S + D (B)	353947	745942
Inlet	S + D (C,D)*	637582	1375829
Outlet	S + D (C,D)*	515009	1096778

*Direct addition of dynamic load components.

As can be seen, all loads are acceptable.

Condition notes:
S = Static
D = Dynamic
(B) = Service Level B
(C) = Service Level C
(D) = Service Level D

ITEM 22:

With respect to Section 7.4.3.2.1 of the PUAR (5), provide and justify all dynamic amplification factors used in the calculation of safety-relief valve discharge-induced fluid drag forces on the safety-relief valve system.

RESPONSE:

Safety-relief valve (S/RV) discharge-induced fluid drag forces were applied pseudo-statically to the S/RV system. The TQFORBF computer code was used with S/RV line input properties that would produce the highest force amplitudes possible from any line for any S/RV discharge case. Maximum amplitude force-time histories were thus determined. From these time histories, the peak amplitudes of the distributed forces were taken for equivalent static application to the system.

The equivalent pseudo-static force distribution was determined by conservatively assuming the distribution of peak forces to act as a perfectly steady-state sinusoidal forcing function. A modal analysis of the S/RV system indicated that there were no potentially responsive modes of the system within the broadened 4.2-14.7 Hz range (see PUAR Section 5.5.2) of possible S/RV forcing frequencies. Therefore, the lowest potentially responsive natural frequency of the system was assumed to be driven by the highest possible broadened forcing frequency of each load case considered. This pulls the two frequencies (i.e., the forcing frequency and the system frequency) as close together as they can ever possibly be, thereby conservatively maximizing the dynamic load factor (DLF). The DLF was computed for each S/RV load case considered using the following expression for a harmonic forcing function (see PUAR Equation D.1.2-24):

$$DLF = \frac{1}{(1 - \Omega^2/\omega^2)^2 + 4\,(\zeta\Omega/\omega)^2}$$

where

ζ = damping ratio (2% was used)

Ω = forcing function frequency

ω = system natural frequency

The load cases considered and corresponding DLFs were as follows:

Case No.	Description	Ω (Hz)	ω (Hz)	DLF
1	NOC,DBA-1st Actuation	8.34	18.25	1.26
2	NOC,DBA-2nd Actuation	10.29	18.25	1.46
3	SBA,IBA-1st Actuation	12.31	18.25	1.84
4	SBA,IBA-2nd Actuation	14.69	18.25	2.83

Finally, BFN S/RV test results showed significant conservatism of S/RV discharge line and support stresses relative to analytically predicted values. See PUAR Sections C.7.1 and C.7.2.

ITEM 23:

With respect to Section 8.2.2.3 of the PUAR (5), provide and justify the reasons for not considering the contributions of higher modes above 20 Hz for seismic analysis of torus attached piping systems.

RESPONSE:

Seismic analysis of torus-attached piping systems was performed using the original analysis methodology as permitted by Section 4.4.1 of NUREG 0661. Original seismic piping analysis methodology of BFN documented in FSAR Appendix C.3.2.1.a, includes use of 20 Hz as the "cut-off" frequency.

ITEM 24:

With respect to Section 8.2.5.2 of the PUAR (5), provide justification for considering branch lines having peak spectral accelerations below 5.0 g at the point of attachment to the process line to be qualified without further evaluation.

RESPONSE:

TVA's criteria for excluding branch lines from additicnal analysis may have been misinterpreted. The exclusion limit is not the acceleration input to the branch line from the process line. It is the amplified motion of the process line, i.e., the exclusion limit is based on the dynamic reponse spectra for the branch line.

The 5-g limit was originally selected based on TVA's experience with seismic qualification of small lines with typical BFN configurations. Experience with BFN LTP analysis of branch lines which exceeded the 5-g limit provided further verification of the acceptability of this limit for BFN branch lines.

ADDENDUM

During the September 13, 1984 meeting, FRC representatives indicated some concern with this response and during a telecon on September 24, 1984, additional information was requested. That information follows:

All branch lines which connect to the torus attached piping process lines were evaluated for dynamic response of the branch line, thermal and dynamic displacement of the attached process line, and sustained loads (deadweight and pressure). Referring to paragraph NC3650 of the 1977 ASME Section III Code (PUAR Reference 23), branch line dynamic response stresses plus sustained load stresses are included in code equation 9, whereas branch line stresses due to process line displacements and sustained loads are included in equation 11.

The 5-g limit for branch line dynamic response analysis was specified on the basis of experience as described above. The adequacy of that limit and the fact that equation 11

stresses are typically more critical for BFN branch lines than equation 9 stresses is shown by Table FRC-24-1. That tabulation gives results for ten BFN Unit 3 branch lines which had response spectra exceeding the 5-g limit. Stresses are presented as a percentage of the code equation 9 and 11 allowables. The peak of response spectra accelerations and branch line identifiers are also given.

Recognizing that the equation 11 stresses were more critical, all branch lines were analyzed for these conditions. It was not necessary or cost effective to rigorously analyze all branch lines for equation 9 stresses--hence the 5-g limit.

Finally, the small compact valves which are located in BFN branch lines are structurally adequate for accelerations much greater than 5-g's. Therefore, the 5-g limit is also appropriate from a component operability standpoint.

TABLE FRC-24-1

TYPICAL BRANCH LINE ANALYSIS RESULTS

Process Line Penetration	Process Line Node Point	Fraction of Allowable Stress		Peak Spectral Acceleration, g's
		Equation 11	Equation 9	
X212	37	.3	.3	9.5
	30	.9	.1	6.1
	40	.1	.1	9.3
	46	.1	.1	6.3
	107	.4	.3	9.9
X214	55	.4	.1	9.5
X223B	E30	.2	.1	10.8
X231	55	.6	.4	9.9
	75X	.2	.1	20.1
	75Z	.5	.2	20.1

ITEM 25:

With respect to Section 8.2.5.5 of the PUAR (5), provide justification for considering the valves with accelerations less than 3-g horizontal and 2-g vertical and having no operator supports to be qualified without further evaluation.

RESPONSE:

The 3-g horizontal and 2-g vertical acceleration limits on valve accelerations are justified by our experience with seismic qualification of similar valves on four TVA nuclear plants (Browns Ferry, Sequoyah, Watts Bar, and Bellefonte). In addition, none of the numerous valves which were evaluated for the BFN LTP had any problem with satisfying the requirements of PUAR Section 4.3.3 with applied accelerations in excess of the 3-g/2-g limits.

ITEM 26:

Provide a schedule for the completion of pipe support modifications for Units 2 and 3.

RESPONSE:

The BFN Unit 1 and Unit 3 pipe support modifications are complete, and all Unit 2 internal pipe support modifications are complete.

An integrated modification schedule was submitted in August 1984 for NRC review and approval, indicating completion of Unit 2 external pipe support modifications during the Cycle 6 refueling outage. That schedule was subsequently revised to show completion of all Unit 2 modifications during the Cycle 5 refueling outage.

Therefore, all BFN LTP pipe support modifications will be installed before restart for Cycle 6 operations in accordance with NRC's orders (PUAR Reference 12).